Pivoting through the chiral-clock family

Nick G. Jones[1⋆], Abhishodh Prakash[2,3†] and Paul Fendley[4‡]

1 St John's College and Mathematical Institute, University of Oxford, UK
2 Rudolf Peierls Centre for Theoretical Physics, University of Oxford, UK
3 Harish-Chandra Research Institute, Prayagraj (Allahabad), India
4 All Souls College and Rudolf Peierls Centre for Theoretical Physics, University of Oxford, UK

⋆ nick.jones@maths.ox.ac.uk , † abhishodhprakash@hri.res.in ,
‡ paul.fendley@physics.ox.ac.uk

Abstract

The Onsager algebra, invented to solve the two-dimensional Ising model, can be used to construct conserved charges for a family of integrable N-state chiral clock models. We show how it naturally gives rise to a "pivot" procedure for this family of chiral Hamiltonians. These Hamiltonians have an anti-unitary CPT symmetry that when combined with the usual $\mathbb{Z}_N$ clock symmetry gives a non-Abelian dihedral symmetry group D_{2N}. We show that this symmetry gives rise to symmetry-protected topological (SPT) order in this family for all even N, and representation-SPT (RSPT) physics for all odd N. The simplest such example is a next-nearest-neighbour chain generalising the spin-1/2 cluster model, an SPT phase of matter. We derive a matrix-product state representation of its fixed-point ground state along with the ensuing entanglement spectrum and symmetry fractionalisation. We analyse a rich phase diagram combining this model with the Onsager-integrable chiral Potts chain, and find trivial, symmetry-breaking and (R)SPT orders, as well as extended gapless regions. For odd N, the phase transitions are "unnecessarily" critical from the SPT point of view.

1   Introduction

The interplay of symmetries, topology and entanglement results in a zoo of interesting topological phases of quantum matter [1,2]. A particularly useful technique is to map a lattice model with well-understood physics to one with a non-trivial order. Kramers-Wannier (KW) duality [3], for example, relates models belonging to the trivial phase to those with spontaneously broken symmetries. In the setting of symmetry-protected topological (SPT) phases of matter, an analogous role is played by the so-called SPT entangler [4–8]. It is a finite-depth unitary operator that transforms trivial models into non-trivial SPTs characterised by unbroken symmetries and distinguished from the trivial phase by robust boundary modes and topological response to gauge fields.

The *pivot procedure* [7,9] provides a systematic way of constructing such SPT entanglers. Pivot Hamiltonians generate SPT entanglers upon exponentiation, and themselves have long-range order. Adding them to trivial and SPT Hamiltonians[1] produces a rich phase diagram.

---

[1]A Hamiltonian belonging to the trivial phase has a unique ground state that can be smoothly connected to a product state without breaking symmetry. Hamiltonians belonging to non-trivial SPT phases have unique ground states in the absence of boundaries but cannot be adiabatically connected to a product state along a symmetric path. Note that we consider the zero temperature phase diagram and so classifying gapped 'parent' Hamiltonians and their ground states is equivalent [10]. Key notions are reviewed in [2,5,11–13].
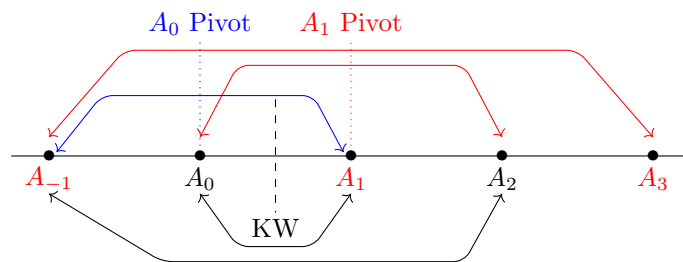
Figure 1: Web of maps generated by pivoting and Kramers-Wannier duality in the Onsager-integrable chiral-clock family.

Analysing this structure allows a deeper understanding of how various quantum orders are intertwined in the phase diagrams of lattice models. The key example of [7,9] starts with the transverse-field Ising chain (i.e. a qubit chain) and yields the cluster model Hamiltonian [14] describing a non-trivial SPT phase [15].

We show how the pivot procedure in this case follows directly from the *Onsager algebra*, introduced by Onsager to compute the free energy of the 2D classical Ising model [16] and the spectrum of the corresponding quantum chain. This infinite-dimensional Lie algebra is constructed by splitting the transverse-field Ising Hamiltonian into two pieces A_0 and A_1, the former coupling to the transverse field and the latter the nearest-neighbour interaction. As we explain below, the other generators are found by taking repeated commutators with these two [17,18], and imposing the Dolan-Grady relations [19].

The Onsager algebra is all that is needed to implement this pivot procedure. Any pair of Hamiltonians generating an Onsager algebra will satisfy the same pivot relations, and resulting Hamiltonians are given by the same simple closed-form expressions in terms of the Onsager generators. The explicit expressions of the Hamiltonians in terms of the the usual qudit operators may be rather nasty, but combining the pivot procedure with the Onsager algebra allows us to derive important physical properties in a simple and systematic fashion. Whether the starting Hamiltonian is of pivot type in the sense of Ref. [7] depends on whether the procedure results in an SPT model for an appropriate symmetry group.

A beautiful presentation of the Onsager algebra is provided by a set of $\mathbb{Z}_N$-invariant clock chains [17,20,21]. Namely, the "superintegrable chiral Potts" chain [22] also can be split into two pieces that generate the identical algebra. For $N > 2$ the algebra is not sufficient to solve the model, but it can be used to construct a sequence of commuting charges. These charges indicate the chain with periodic boundary conditions is integrable.

In this paper, we exploit the connection between pivoting and the Onsager algebra to apply the pivot procedure to this family of Onsager-integrable clock Hamiltonians. The resulting Hamiltonians are related by both pivoting and Kramers-Wannier duality, as illustrated in Fig. 1. We show that the global symmetry for a given N is the dihedral group D_{2N}, arising from the $\mathbb{Z}_N$ clock symmetry along with an anti-unitary CPT symmetry. One key consequence of the pivot procedure is that non-trivial models (for example with symmetry fractionalisation) can arise by unitarily transforming from models with easy-to-understand behaviour. For example, taking A_0 to be the Hamiltonian yields a trivial paramagnet, while taking A_1 induces spontaneous symmetry breaking. The Hamiltonian A_2 is generated by pivoting A_0 with A_1. For $N = 2$ these correspond to the familiar Ising paramagnet and ferromagnet respectively, while A_2 is the cluster Hamiltonian with SPT order (see Eq. (6) below).

One of the main results of this paper is a demonstration that for any even N, A_2 describes an SPT phase. For odd N, it describes a "representation SPT" (RSPT) [23], similar to what occurs in even-spin Haldane phases [24]. RSPTs do not enjoy the same topological protection as SPTs, but nevertheless have some similar phenomenology [25].

Both SPT and RSPT phases exhibit symmetry fractionalisation, but only for the former are the representations projective. The dominant Schmidt eigenvalues for both form a doublet, but only for the former do all eigenvalues pair. Thus the SPT at even N disappears only when parameters are tuned through a bulk phase transition. For odd N, however, the RSPT can disappear [25] at a boundary transition or at an "unnecessary" bulk transition [26–32]. (For our purposes, we say that a ground state is an RSPT when the dominant Schmidt eigenvalues have a degeneracy due to a non-trivial linear irreducible representation of the non-Abelian symmetry.) Connecting the various Hamiltonians yields interesting phase diagrams. We find (R)SPT phases and extended gapless phases as well as more conventional disordered and spontaneous symmetry broken phases. The interpolation $H = A_1 + \lambda A_0$ is the familiar transverse-field Ising model for $N = 2$ and corresponds to the "superintegrable chiral Potts" chain for $N \geq 3$ [20,33]. The latter, at least for $N = 3$, contains extended gapless phases [34,35]. Hamiltonians that connect A_0, A_1, A_2 exhibit an even richer phase diagram, for example including symmetry-enriched critical points for $N = 2$ [6,36]. Another result of ours is to show that for $N = 3$ and $N = 4$ this model hosts a variety of strongly correlated gapped and gapless states. For any linear combination of the A_k, the model is presumably integrable, as it possesses an infinite set of local and mutually-commuting charges [21]. However, utilising integrability in chiral clock models requires a rather intricate analysis, and we defer it to a separate paper [37].

The paper is organised as follows. In Section 2, we introduce both the pivot procedure and the Onsager algebra, and show that implementing the former follows directly from building Hamiltonians from the generators of the latter. In Section 3 we introduce the chiral-clock family of Hamiltonians and its Onsager-algebra structure. We find its symmetries and ground states, in particular the matrix-product state ground state for A_2. In Section 4 we show that SPT and RSPT phases occur at even and odd N respectively, all exhibiting symmetry fractionalisation. In Section 5 we discuss the phase diagram of the combined Hamiltonian $\alpha A_0 + \beta A_1 + \gamma A_2$, illuminating how the distinct phases fit together. Finally, we detail some natural questions for future work.

2 Pivoting with Onsager

2.1 What Onsager did

Onsager's solution of the two-dimensional classical Ising model with periodic boundary conditions [16] is a tour de force. He computed the full spectrum of the transfer matrix, and hence the exact partition function. Taking a strongly anisotropic limit then yields the exact spectrum of the corresponding quantum Hamiltonian of the transverse-field Ising chain.

The core of Onsager's result comes from understanding the algebra obeyed by the generators of the Hamiltonian and transfer matrix. These generators are written in terms of Pauli matrices acting on the usual Hilbert space of L two-state systems, i.e. $(\mathbb{C}^2)^{\otimes L}$. The two basic generators are

$$A_0 = -\sum_{j=1}^{L} \sigma_j^x, \qquad A_1 = -\sum_{j=1}^{L} \sigma_j^z \sigma_{j+1}^z, \tag{1}$$

where in the latter $\sigma_{L+1}^z \equiv \sigma_1^z$. The transverse-field Ising Hamiltonian with periodic boundary conditions is then simply $H_I = A_0 + \lambda A_1$.

Other generators of the Onsager algebra are found by taking commutators of the basic two, subject to two key identities. Onsager showed by explicit computation that

$$\left[A_1, \left[A_1, [A_1, A_0]\right]\right] = 16[A_1, A_0], \qquad \left[A_0, \left[A_0, [A_0, A_1]\right]\right] = 16[A_0, A_1]. \tag{2}$$

Imposing these identities, now known as the Dolan-Grady conditions, results in an infinite-dimensional Lie algebra, canonically represented by a set of generators $\{A_l, G_m | l, m \in \mathbb{Z}\}$, with $G_{-k} = -G_k$ and $G_0 = 0$. The next two generators are defined by

$$G_1 = \tfrac{1}{4}[A_1, A_0], \qquad A_2 = A_0 - \tfrac{1}{2}[A_1, G_1], \tag{3}$$

so that the first Dolan-Grady condition can be written as $[A_1, A_2] = [A_0, A_1]$. With A_0 and A_1 defined by (1), $A_2 = \sum_j \sigma_{j-1}^z \sigma_j^x \sigma_{j+1}^z$ results. (Here and henceforth all sums over j run from 1 to L.) Proceeding in this fashion, Onsager defined and found explicit expressions for all the generators, and showed that they satisfy

$$\boxed{[A_l, A_m] = 4G_{l-m}, \qquad [G_l, A_m] = 2A_{l+m} - 2A_{m-l}, \qquad [G_l, G_m] = 0.} \tag{4}$$

A quicker way of establishing (4) for A_0 and A_1 from (1) is by rewriting them in terms of Majorana-fermion bilinears by using the Jordan-Wigner transformation. A commutator of fermion bilinears always yields a bilinear, so all the Onsager generators in this representation can be written as fermion bilinears. Explicit expressions and other useful details may be found in e.g. [38].

The exact spectrum of H_I follows from the Onsager algebra (4) because of a crucial simplification of the presentation (1). As there are only $L(2L-1)$ possible fermion bilinears on L sites, there can be at most $2L-1$ distinct generators of (4) (by construction all generators are translation invariant). Indeed, $A_{l+L} = \pm A_l$ and $G_{l+L} = \pm G_l$, where the sign can be found in [16] (or working out the explicit fermion-bilinear expressions). To find the spectrum, one then can reduce the spectrum of H_I to a sum by taking the Fourier transformation of the Onsager generators.

Such a simplification does *not* occur in the chiral-clock presentations of the Onsager algebra that we study. As we describe below, however, the Onsager algebra provides a systematic way of constructing pivot Hamiltonians, making it useful in any presentation.

2.2 The Ising pivot

The pivot procedure provides a method for generating SPT phases via unitary transformations [7,9]. One starts with a Hamiltonian H_0 with a trivial (product state) ground state and then searches for a local "pivot" Hamiltonian H_{pivot} that yields an SPT Hamiltonian via

$$H_{\text{SPT}} = U(\pi) H_0 U(\pi)^\dagger, \qquad U(\theta) = \exp(-i\theta H_{\text{pivot}}). \tag{5}$$

The simplest example comes from the Ising Hamiltonian (1). Taking $H_0 = A_0$ from there gives a trivial paramagnetic phase with a unique ground state. Defining $H_{\text{pivot}} = A_1/4$ from (1) then gives

$$H_{\text{SPT}} = e^{-i\pi A_1/4} A_0 \, e^{i\pi A_1/4} = \sum_j \sigma_{j-1}^z \sigma_j^x \sigma_{j+1}^z = A_2. \tag{6}$$

All three of these Hamiltonians have a $\mathbb{Z}_2 \times \mathbb{Z}_2^T$ symmetry, generated by the spin-flip $\prod_j \sigma_j^x$, and complex conjugation in the Z-diagonal basis. This symmetry protects the SPT order (see Section 4.1 for details).

The Hamiltonian $-H_{\text{SPT}}$ is the canonical cluster model [14], and both $\pm H_{\text{SPT}}$ exhibit SPT order. (The sign can be toggled by conjugating by $\prod_k \sigma_{4k}^x \sigma_{4k+1}^x$ [7].) Stated differently, $\exp(-i\pi A_1/4)$ is the cluster SPT entangler.[2] Since the ground state of A_0 is a product state

---

[2]The fact that the ground state of the cluster model can be generated via a finite-time evolution generated by Ising-like Hamiltonians is well known from the study of measurement-based quantum computing (MBQC) [39]. In this context the cluster state, as well as other SPT ground states, serves as a good resource state [40–43].

and the terms in A_1 are all mutually commuting, the ground state of A_2 can be written as a matrix-product state (MPS) with bond dimension two. Continuing in this fashion allows us to generate an infinite family called the (generalised) cluster models [5, 44–49]. For example, pivoting H_{SPT} with H_0 gives another (SPT) spin chain with Hamiltonian $\sum_j \sigma^y_{j-1} \sigma^x_j \sigma^y_{j+1}$. Since A_0 and A_1 from (1) can be written in terms of fermion bilinears, all Hamiltonians generated in this fashion are written as bilinears. They all can thus be easily solved via standard techniques.

In general, the pivot procedure [7] works as follows. The starting point is a Hamiltonian H_0 with symmetry group G, and a product state for its unique ground state. Considering the one-parameter deformation $H(\theta) = e^{-i\theta H_{\text{pivot}}} H_0 e^{i\theta H_{\text{pivot}}}$, we *require* that $H(2\pi) = H(0)$, and that $H(\pi)$ is a non-trivial SPT phase protected by the group G. This means that, for $U(\theta) = \exp(-i\theta H_{\text{pivot}})$, $U(2\pi)$ is a symmetry of H_0, while $U(\pi)$ acts as an SPT entangler. In our analysis below we broaden this picture to include multiple generalisations of the Ising pivot including where $U(\pi)$ is not an SPT.

2.3 Pivoting with Onsager

Here we show that constructing pivots of this type does *not* require the explicit representation (1), but only the Onsager algebra. Given *any* lattice Hamiltonian realisation of A_0 and A_1 satisfying the Dolan-Grady relations, we show how pivoting generates a family of Hamiltonians with a simple closed form in terms of the Onsager generators. We here prove this fact, and in the rest of the paper exploit it.

The connection between the two procedures is rather direct. Indeed, when A_0 and A_1 are defined by (1), A_2 from the Onsager definition (3) is equal to H_{SPT} from (6). The latter equation thus implies that A_2 can be found by pivoting with $A_1/4$, i.e.

$$A_2 = e^{-i\pi A_1/4} A_0\, e^{i\pi A_1/4}\,. \tag{7}$$

This relation follows directly from the Onsager algebra, and is a particular case of the general identity (see [17, 50] for related results)

$$e^{-i\alpha A_m} A_l\, e^{i\alpha A_m} = \cos^2(2\alpha) A_l + \sin^2(2\alpha) A_{2m-l} + i\sin(4\alpha) G_{l-m}\,. \tag{8}$$

To prove (8), we first use the Onsager algebra to generalise the Dolan-Grady relations to

$$\Big[\big[[A_l, A_m], A_m\big], A_m\Big] = 4\Big[[G_{l-m}, A_m], A_m\Big] = 8[A_l - A_{2m-l}, A_m] = 32\, G_{l-m} = 16[A_l, A_m]\,. \tag{9}$$

Using the standard identity [51]

$$e^{-B} C e^{B} = \sum_{p=0}^{\infty} \frac{1}{p!} \underbrace{\Big[\big[[C, B], B\big], \ldots, B\Big]}_{p-\text{fold}} \tag{10}$$

with (9) yields

$$e^{-i\alpha A_m} A_l e^{i\alpha A_m} = A_l + [A_l, A_m] \sum_{n=1}^{\infty} \frac{(i\alpha)^{2n-1}}{(2n-1)!} 16^{n-1} + [[A_l, A_m], A_m] \sum_{n=1}^{\infty} \frac{(i\alpha)^{2n}}{(2n)!} 16^{n-1}\,.$$

The two sums are $i\sin(4\alpha)/4$ and $-\sin^2(2\alpha)/8$ respectively, and using (4) to rewrite the remaining commutators yields (8).

The identity (8) yields a sequence of exact pivot relations, with no further computations necessary. Defining $U_m(\theta) = e^{-i\theta A_m/4}$ yields

$$U_m(\pi) A_l\, U_m(\pi)^{\dagger} = A_{2m-l}\,, \qquad U_m(2\pi) A_l\, U_m(2\pi)^{\dagger} = A_l\,. \tag{11}$$

All A_l thus can be generated by a sequence of pivots with A_0 and A_1:

$$A_{l+2} = U_1(\pi)U_0(\pi)A_l\,U_0(\pi)^\dagger U_1(\pi)^\dagger, \qquad A_{-l} = U_0(\pi)A_l\,U_0(\pi)^\dagger. \tag{12}$$

The A_l thus fall into an even and an odd family, unitarily equivalent to A_0 and A_1 respectively. The two families are themselves related by a duality $A_n \to A_{1-n}$ that preserves the algebra (in the chiral clock family this is a KW duality [52], see Fig. 1). Moreover, any unitary symmetry commuting with A_0 and A_1 commutes with all the A_l. The same holds for anti-unitary symmetries, because using $U_m(-\pi)$ in Eq. (11) yields the same action on the A_l.

This construction immediately gives us information about the phase structure. Suppose that A_0 is a representative of the trivial phase. Then A_{2k} necessarily has a unique ground state for all k, i.e., there is no symmetry breaking in the ground state. If A_{2k} is a non-trivial SPT for some value of k, Eq. (11) tells us immediately that $A_k/4$ is a pivot Hamilton giving the SPT entangler for this model. Moreover, the pivot Hamiltonian itself generates a symmetry of the 'halfway point' between the starting model and the pivoted model:

$$\left[A_l, A_{l-m} + A_{l+m}\right] = 4G_{-m} + 4G_m = 0. \tag{13}$$

In our examples, all A_l have integer eigenvalues and so generate a $U(1)$ symmetry.

3 The integrable chiral clock chains

In this section we give a set of chiral Hamiltonians satisfying the Onsager algebra, and explore their basic properties using pivoting. We exploit the fact that the Onsager algebra automatically follows from any A_0 and A_1 obeying Dolan-Grady conditions; the remainder of the relations are simply definitions and consistency conditions [17–20]. Thus any Hamiltonian built from Onsager-algebra generators A_l possesses an elegant pivot structure, i.e. any model obeying (2) automatically satisfies (11). We emphasise that although the chains are integrable, they are *not* free-fermionic.

3.1 Onsager and the integrable chiral clock models

We study Hamiltonians generated by two pieces of the "superintegrable chiral Potts" Hamiltonian chain [17, 18, 20, 21]. These pieces satisfy the Dolan-Grady relations and hence generate the Onsager algebra. We call this set of chains the Onsager-integrable chiral-clock family.[3] The Hilbert space is a chain of N-state quantum systems, i.e. $\left(\mathbb{C}^N\right)^{\otimes L}$, acted on by "shift" and "clock" operators generalising Pauli matrices. Each such operator X_j, Z_j acts non-trivially on a single site j of the chain, and they obey $X_j Z_k = \omega^{\delta_{jk}} Z_k X_j$, along with $(X_j)^N = (Z_j)^N = 1$. In the Z-diagonal basis they act on the jth site as

$$X_j = \sum_{a_j=0}^{N-1} \left|a_j - 1\right\rangle\left\langle a_j\right|, \qquad Z_j = \sum_{a_j=0}^{N-1} \omega^{a_j} \left|a_j\right\rangle\left\langle a_j\right|, \tag{14}$$

while leaving other sites unchanged. We have defined $\omega = e^{2\pi i/N}$ and identify basis states modulo N, i.e. $|a\rangle \equiv |a \bmod N\rangle$. For $N=2$ they reduce to the corresponding Pauli operators σ_j^x, σ_j^z.

We build our Hamiltonians from the operators

$$h_{2j-1} = X_j, \qquad h_{2j} = Z_j^{-1} Z_{j+1}, \tag{15}$$

---

[3]We call them "clock" instead of "Potts" chains because the latter typically have S_N symmetry that ours do not possess. We use "Onsager-integrable" instead of "superintegrable" as the former is more specific.

where the site-index j on the right-hand-side is, as always, defined mod L. These operators obey $\omega h_k h_{k+1} = h_{k+1} h_k$ and commute otherwise. The Onsager generators are then

$$A_0 = -\frac{4}{N} \sum_j \sum_{m=1}^{N-1} \alpha_m (h_{2j-1})^m, \qquad A_1 = -\frac{4}{N} \sum_j \sum_{m=1}^{N-1} \alpha_m (h_{2j})^m, \qquad \alpha_m = \frac{1}{1-\omega^m}. \quad (16)$$

For $N = 2$ these reduce to (1). This presentation is "self-dual" in that A_0 and A_1 are related by Kramers-Wannier duality. This duality here shifts all $h_k \to h_{k+1}$ and so exchanges A_0 and A_1. Since the algebra of the h_m is invariant under this shift, one Dolan-Grady condition implies the other. The "superintegrable chiral Potts" Hamiltonian is $H(\lambda) = A_1 + \lambda A_0$; it is an anisotropic limit of the 2D classical "chiral Potts" model [17, 22, 53, 54].

The operators from (16) satisfy the Dolan-Grady conditions (2) and hence generate the full Onsager algebra (4) for any N [20]. We review this calculation in Appendix A. Closed-form expressions for the generators in general, however, are not known, as the explicit expressions get rather nasty beyond the first few. Expressions for A_{-1} can be found in [21, 38]. The expression for A_2 is found by using duality from A_{-1}, pivoting using (7), or simply working out the commutators from the definition (3). We present the calculations in Appendix A; see also [17]. The nicest way to write the result is as

$$A_2 = -\frac{4}{N} \sum_j \sum_{m=1}^{N-1} \alpha_m S_{j-1,j}^{(m)} X_j^m S_{j,j+1}^{(m)},$$

$$S_{j-1,j}^{(m)} = 1 - \frac{2m}{N} - \frac{2}{N} \sum_{m'=1}^{N-1} \alpha_{m'} (1 - \omega^{mm'}) Z_{j-1}^{-m'} Z_j^{m'}. \quad (17)$$

A key feature of this form is that $S_{j-1,j}^{(m)}$ has eigenvalues ± 1. Thus despite its complicated-looking definition, in the Z-basis this operator is diagonal with entries ± 1. The expression for A_{-1} is found simply by writing these expressions in terms of the h_k and then shifting $h_k \to h_{k+1}$.

The Onsager relations mean that any linear combination of the A_l possesses an infinite sequence of local and mutually commuting charges [21], i.e.

$$\mathcal{H} \equiv \sum_{k=a}^{b} t_k A_k, \qquad Q_m \equiv \sum_{k=a}^{b} t_k (A_{m+k} + A_{-m+k}) \quad \Longrightarrow \quad [\mathcal{H}, Q_m] = 0. \quad (18)$$

The existence of this sequence implies that any such model is integrable. These conserved charges do not exhaust the symmetries of $\mathcal{H}$. A $U(1)$-invariant Hamiltonian that commutes with all the Onsager generators was discussed in depth in [38]. Thus $\mathcal{H}$ commutes with this Hamiltonian, meaning the latter can be thought of as an additional conserved charge. Another symmetry is the dihedral symmetry discussed next.

3.2 Dihedral symmetry

The appearance of a larger non-Abelian symmetry group in chiral clock models is known; see e.g. [35, 55–58]. We describe its most general form here. The generators of the Hamiltonians are all invariant under the $\mathbb{Z}_N$ symmetry generated by

$$r = \prod_j X_j \qquad \Longrightarrow \qquad h_k r = r h_k. \quad (19)$$

Less obviously, the symmetry extends to the dihedral group D_{2N}, whose generators obey

$$D_{2N} \cong \langle r, s | r^N = s^2 = 1, \; srs = r^{-1} \rangle. \quad (20)$$

The second generator s implements CPT symmetry here. We define P to be spatial inversion, exchanging site j with $L + 1 - j$. (The particular choice of fixed site or bond is arbitrary in a translationally invariant system.) Charge conjugation C is defined so that $CX_j C^\dagger = X_j^\dagger$ and $CZ_j C^\dagger = Z_j^\dagger$ for all j. In the Z-diagonal basis it is

$$C = \prod_j C_j, \qquad \text{where} \quad C_j = \sum_{a=0}^{N-1} |a_j\rangle\langle N - a_j|. \tag{21}$$

Time reversal is implemented by an anti-unitary operator $\mathcal{K}$ that we define as complex conjugation in the Z-basis. It is simple to check that $s = CP\mathcal{K}$ is a symmetry of all our chiral-clock Hamiltonians:

$$sA_0 s = A_0, \qquad sA_1 s = A_1 \qquad \Longrightarrow \quad sA_l s = A_l. \tag{22}$$

The dihedral symmetry will prove crucial in our analysis of the phases of these Hamiltonians.

3.3 Maps amongst the family

One key observation in Ref. [7] is that the pivoting relation in the cluster models gives us a large number of mappings between models. Since we showed that the unitary transformations (11) follow solely from the Onsager algebra, pivoting with A_m thus unitarily transforms any $A_l \to A_{2m-l}$. Hence, visualising the space of models $\{A_k\}$ as points on a line, pivoting with A_m corresponds to reflection around each point m. Combining two pivots as in e.g. (12) gives a unitary transformation that shifts the index $A_l \to A_{l+2}$, as illustrated in Fig. 1.

As indicated above, Kramers-Wannier duality maps $A_0 \to A_1$ and vice versa. The Onsager algebra then requires that sending $A_0 \to A_1$ maps $A_n \to A_{1-n}$. In Fig. 1, this map corresponds to reflection about the bond between A_0 and A_1. Some care must be taken: Kramers-Wannier duality is not invertible, and so is not a one-to-one map. Indeed, we show explicitly below that the ground state of A_1 (and hence all A_l for odd l) is N-fold degenerate, while the ground state of A_0 is unique.

Other operators allow us to relate different models. The anti-unitary operator $\mathcal{V} = \left(\prod_j Z_j \right) \mathcal{K}$ obeys

$$\mathcal{V}^2 = (-1)^L, \qquad \mathcal{V}A_{2k+1} = A_{2k+1}\mathcal{V}, \qquad \mathcal{V}A_{2k} = -A_{2k}\mathcal{V}. \tag{23}$$

There is a unitary operator with the same commutation/anticommutation property [35]. When $L = 0 \bmod N$ the unitary operator $\mathcal{W} = P\prod_j X_j^j$ obeys [35]

$$\mathcal{W}^2 = 1, \qquad \mathcal{W}A_{2k+1} = -A_{2k+1}\mathcal{W}, \qquad \mathcal{W}A_{2k} = A_{2k}\mathcal{W}. \tag{24}$$

Combining the two shows that the spectrum of any linear combination of the A_l is symmetric about zero when L is a multiple of N. Moreover, the spectrum of $\mathcal{H} = \sum_l t_l A_l$ is invariant under sending all $t_{2k} \to -t_{2k}$.

3.4 Ground states

Thanks to the Onsager algebra and the pivot relations, determining the ground state(s) of any Hamiltonian A_l is straightforward.

Although they look rather complicated in their definition, the operators A_0 and A_1 individually take on a simple form in the right basis [17, 20]. The eigenvectors of X_j are

$$\left| v_j^{(n)} \right\rangle = \frac{1}{\sqrt{N}} \sum_{a_j=0}^{N-1} \omega^{-na_j} |a_j\rangle \quad \Longrightarrow \quad X_j \left| v_j^{(n)} \right\rangle = \omega^{-n} \left| v_j^{(n)} \right\rangle, \tag{25}$$
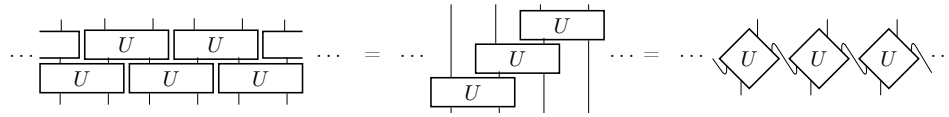
Figure 2: Graphical representations of $U_1(\pi)$ as products $U_{j,j+1}$ from (30). The left-hand picture is a depth-two local unitary circuit, the middle a staircase circuit. The latter can be interpreted as an MPU with bond-dimension N (right).

so the eigenvectors of A_0 are simply product states

$$A_0 \prod_j \left| v_j^{(n_j)} \right\rangle = E_0(\{n_j\}) \prod_j \left| v_j^{(n_j)} \right\rangle, \qquad \text{where } E_0(\{n_j\}) = -\frac{4}{N} \sum_{j=1}^{L} \sum_{m=1}^{N-1} \alpha_m \omega^{-mn_j}, \quad (26)$$

for any choice of the $n_j = 0,\dots,N-1$. The eigenvalues simplify using the trigonometric identity

$$\sum_{m=1}^{N-1} \alpha_m \omega^{-mn} = \frac{(N-1)}{2} - n, \qquad 0 \le n \le N-1, \quad (27)$$

so that

$$E_0(\{n_j\}) = -2L \frac{N-1}{N} + \frac{4}{N} \sum_j n_j. \quad (28)$$

Hence the unique ground state of A_0 has all $n_j = 0$, yielding a trivial paramagnet. Worth noting is that the full spectrum is invariant under $E_0 \to -E_0$, and that all eigenvalues are integers up to the shift and the overall factor of $4/N$.

Any basis state in the Z-diagonal basis is an eigenstate of A_1. Denoting the eigenvalue of Z_j on each site as ω^{a_j}, using (27) gives the eigenvalue of A_1 to be

$$E_1 = -2L \frac{N-1}{N} + \frac{4}{N} \sum_j \left((a_j - a_{j+1}) \bmod N \right). \quad (29)$$

We emphasise that each term in this sum is taken mod N, as a consequence of the restriction in (27). The energy E_1 from (29) is invariant under shifting all $a_j \to (a_j + m) \bmod N$ for any m, so each level is N-fold degenerate. The N ground states of A_1 are therefore given by setting $a_j = a$ for all j. These ferromagnetic ground states spontaneously break the $\mathbb{Z}_N$ symmetry r.

The operators A_l for even and odd l are unitarily equivalent to A_0 and A_1 respectively, as follows from the pivot relation (12). Thus A_l has a unique ground state for l even, while for odd l it has an N-fold ground-state degeneracy. Moreover, since U_0 is a product of on-site unitary operators, it can be thought of as a matrix-product unitary operator (MPU) of bond-dimension zero. For the operator U_1, we exploit the fact that A_1 is a sum of commuting terms. Then $U_1(\pi) = \exp(-i\pi A_1/4)$ can be written as a product of two-site unitaries as

$$U_1(\pi) = \prod_j U_{j,j+1}, \qquad U_{j,j+1} \equiv \exp\left(i \frac{\pi}{N} \sum_{m=1}^{N-1} \frac{1}{1-\omega^m} Z_j^{-m} Z_{j+1}^m \right). \quad (30)$$

As illustrated in Fig. 2, we can rewrite this product as an MPU of bond-dimension N. Thus the ground states of A_{2k} and A_{2k+1} can each be written as an MPS of bond dimension upper bounded by N^k.

The N-channel MPS for the ground state of A_2 can be put in an elegant form. Using a bit of Fourier transformation along with (27) shows that the MPU tensor acts on the X-basis eigenstates (25) as

$$U_{j,j+1} \left| v_j^{(s)} v_{j+1}^{(t)} \right\rangle = \frac{1}{N} \sum_{r=0}^{N-1} \lambda_r \left| v_j^{(s+r)} v_{j+1}^{(t-r)} \right\rangle, \qquad \lambda_r = \frac{\omega^{r/2}}{\sin(\pi(r+\frac{1}{2})/N)}. \quad (31)$$

The ground state of A_2 is thus

$$
\begin{aligned}
|\psi_2\rangle &= U_{L1}\cdots U_{23}U_{12}\left|v_1^{(0)}v_2^{(0)}\cdots v_L^{(0)}\right\rangle \\
&= N^{-L}\sum_{n_1,\ldots,n_L}\left(\prod_{j=1}^{L}\lambda_{n_j}\right)\left|v_1^{(n_1-n_L)}v_2^{(n_2-n_1)}v_3^{(n_3-n_2)}\cdots v_L^{(n_L-n_{L-1})}\right\rangle \\
&= N^{-3L/2}\sum_{a_1,\ldots,a_L}\sum_{n_1,\ldots,n_L}\left(\prod_{j=1}^{L}\lambda_{n_j}\omega^{a_j(n_{j-1}-n_j)}\right)|a_1\cdots a_L\rangle\,,
\end{aligned}
\tag{32}
$$

where all sums run from 0 to $N-1$. Converting the sums over the $\{n_j\}$ into matrix products yields

$$
|\psi_2\rangle = \sum_{a_1,\ldots,a_L}\operatorname{tr}\left(\mathcal{A}_{a_1}\cdots\mathcal{A}_{a_L}\right)|a_1\cdots a_L\rangle\,, \qquad \mathcal{A}_a^{n,n'} = \frac{\lambda_{n'}}{N\sqrt{N}}\omega^{a(n-n')}\,.
\tag{33}
$$

It is straightforward to obtain the entanglement spectrum from this expression, as we discuss in the next section.

4 SPTs and RSPTs in the chiral-clock family

SPT phases are guaranteed to be stable only to perturbations preserving the protecting symmetries. One thus expects there to be a (non-symmetric) finite-depth local unitary transformation from a ground state with SPT order into a trivial product state [59]. The inverse of such a transformation is an SPT entangler [4–8, 60]. SPTs in clock models outside of the chiral family we consider have been studied previously [61, 62], and are interesting because of their relation to deconfined quantum critical points [32, 63–65]. For a general review of SPT physics and for further references, see, for example, Refs. [2, 5, 11–13].

In Section 3.4 we showed how the ground state of A_2 indeed takes the form of a finite-depth local unitary transformation applied to a trivial state. Since we know that this state has SPT order for $N=2$, at least for the symmetry group $\mathbb{Z}_2\times\mathbb{Z}_2^T$ as reviewed in Section 4.1, it is natural to hope that this property holds for all N. The situation, however, is subtler. An SPT with a protecting symmetry group $G=G_0$ or $G=G_0\rtimes\mathbb{Z}_2^{\mathrm{CPT}}$, where G_0 acts on-site, can occur when the group cohomology $H^2(G,U(1))$ is non-trivial [10, 13, 59]. Concretely, this corresponds to the classification of non-trivial projective representations of the symmetry group on the bond indices of an MPS representation of the ground state. The appearance of a non-trivial projective representation corresponds to a non-trivial SPT order. We showed in Section 3.2 that $G=D_{2N}=\mathbb{Z}_N\rtimes\mathbb{Z}_2^{\mathrm{CPT}}$ for our models. Since $H^2(D_{2N},U(1))=\mathbb{Z}_2$ for N even and is otherwise trivial [66], we have the possibility of an SPT protected by this symmetry group only for even N.

In this section, we probe deeper by analysing the properties of the MPS ground state (33) of A_2. In particular, we compute its entanglement spectrum and symmetry fractionalisation. We show that for even N we indeed have SPT order for our D_{2N} symmetry group. For odd N we find that we cannot have SPT order for any protecting symmetry group. However, the ground state has behaviour reminiscent of an SPT, but without being as robust. Such phases were dubbed RSPTs in a closely related context [23], and we discuss how they arise here. For conceptual orientation we will first analyse the cluster model, i.e., the case where $N=2$.

4.1 SPT order in the ground state of A_2 for $N=2$ and symmetry fractionalisation

Projective symmetry fractionalisation in the ground state is characteristic of SPT order. Symmetry fractionalisation is particularly clear in the MPS picture: if two sets of matrices $\mathcal{A}_a$ and

$\mathcal{B}_a$ represent the same state, then $\mathcal{A}_a = e^{i\varphi} M \mathcal{B}_a M^{-1}$ for some phase φ and invertible matrix M on the bonds [67]. For an SPT with a unitary on-site symmetry group G that preserves the ground state, applying a symmetry to the physical index gives us an equivalent state, and the corresponding M are unitary and form a projective representation of G [68]. The cohomology class of the representation classifies the SPT order [10, 13, 24, 59, 66].

Recall the cluster model Hamiltonian $A_2 = \sum_j \sigma^z_{j-1} \sigma^x_j \sigma^z_{j+1}$ from (6). Along with the $\mathbb{Z}_2$ symmetry generated by $\prod_j X_j$ and the $\mathbb{Z}_2^{\text{CPT}}$ symmetry, this model has a $\mathbb{Z}_2^T$ time-reversal symmetry generated by $\mathcal{K}$, complex conjugation in the Z basis. It is well known (see e.g. [7]) that the symmetry $\mathbb{Z}_2 \times \mathbb{Z}_2^T$ protects SPT order in this model, as we show now via non-trivial symmetry fractionalisation[4] of this Abelian group.

Specialising Eq. (33) to $N = 2$ we have that the ground state MPS of the cluster chain has tensor

$$\mathcal{A}_a^{n,n'} \propto (-1)^{a(n-n')} i^{n'}. \tag{34}$$

Let us renormalise $\mathcal{A}$ to make this relation an equality. Consider the action of the on-site symmetry $\prod_j \sigma^x_j$; then, at a fixed site, the tensor after the symmetry action, $\mathcal{B}$ is given by

$$\mathcal{B}_a^{n,n'} = \sum_{a'} \sigma^x_{aa'} \mathcal{A}_{a'}^{n,n'} = (-1)^{(1-a)(n-n')} i^{n'} = \sum_{m,m'} \sigma^z_{nm} \mathcal{A}_a^{m,m'} \sigma^z_{m'n'}. \tag{35}$$

Suppressing bond indices we write $\sum_{a'} \sigma^x_{a,a'} \mathcal{A}_{a'} = \sigma^z \mathcal{A}_a \sigma^z$, and we say the on-site symmetry σ^x has fractionalised as σ^z on the bonds.

Time-reversal acts on the MPS tensor by conjugation [69], and so we have

$$\mathcal{B}_a^{n,n'} = \overline{\mathcal{A}_a^{n,n'}} = (-1)^{a(n-n')}(-i)^{n'} = -i \sum_{m,m'} \sigma^x_{nm} \mathcal{A}_a^{m,m'} \sigma^x_{m'n'}. \tag{36}$$

We then see that since σ^x and σ^z do not commute (and no multiplication of these generators by complex phases will change this), we have a projective representation of $\mathbb{Z}_2 \times \mathbb{Z}_2^T$ on the bonds. This projective representation cannot change without either breaking this symmetry, or tuning through a phase transition.

Below we make the corresponding analysis for our D_{2N} symmetry group for all N. For $N = 2$ this reduces to $\mathbb{Z}_2 \times \mathbb{Z}_2^{\text{CPT}}$ and it is worth noting that this group differs from both the unitary $\mathbb{Z}_2 \times \mathbb{Z}_2$ and the anti-unitary $\mathbb{Z}_2 \times \mathbb{Z}_2^T$ symmetries that typically protect the SPT order of the cluster model [7].

4.2 No SPT for A_2 with odd N

The distinction between odd and even N is apparent in the entanglement spectrum of $|\psi_2\rangle$. Using $\lambda_n = \omega^{n/2} |\lambda_n|$ we write the matrix elements of $\mathcal{A}_j$ from (33) as

$$\mathcal{A}_a^{n,n'} = \Gamma_j^{n,n'} \Lambda_{n'}, \qquad \Gamma_a^{n,n'} \equiv N^{-\frac{1}{2}} \omega^{a(n-n')} \omega^{n'/2}, \qquad \Lambda_{n'} = N^{-1} |\lambda_{n'}|. \tag{37}$$

This MPS is in canonical form [69, 70] because the transfer matrix $T^{n,p;n',p'} = \sum_a \mathcal{A}_a^{n,n'} \overline{\mathcal{A}}_a^{p,p'}$ has dominant right (left) eigenvector $\delta_{n',p'}$ ($\Lambda_n^2 \delta_{n,p}$) with eigenvalue 1. The entanglement spectrum for a bipartition of an open chain is then $\{\Lambda_n^2\}$, where

$$\Lambda_n^{-1} = N \sin\left(\frac{(2n+1)\pi}{2N}\right), \qquad n = 0, 1, \ldots, N-1. \tag{38}$$

---

[4]Note that for groups with a $\mathbb{Z}_2^T$ anti-unitary time-reversal, the SPT classification is a twisted group cohomology. However, for our purposes we simply want to show the cluster state has a non-trivial projective representation of the group on the bond space; for further details see Ref. [13].

A necessary but not sufficient condition for SPT order is an exact degeneracy in the entanglement spectrum [24, 71, 72]. Since the argument of the sine in (38) is symmetric about $\pi/2$, there is indeed a two-fold degeneracy throughout the spectrum for N even. We show in Section 4.3 that this exact degeneracy is a consequence of a projective representation of D_{2N}, implying SPT order.

For N odd, however, the single non-degenerate Schmidt value $\Lambda_{(N-1)/2} = N^{-1}$ means that there is no non-trivial projective representation in the ground state of A_2. This observation is consistent with the lack of $D_{2N} = \mathbb{Z}_N \rtimes \mathbb{Z}_2^{\text{CPT}}$ SPT order for N odd [66]. Moreover, it implies a stronger statement: for N odd, A_2 cannot describe a non-trivial SPT phase, even if we have missed some symmetries. However, as only the lowest Schmidt value for N odd is non-degenerate, we expect that some of the physics is independent of N.

4.3 Symmetry fractionalisation

We will now show how the D_{2N} symmetry fractionalises for all N, resulting in a non-trivial projective representation for even N.

Having given a simple example of symmetry fractionalisation in Section 4.1, we now introduce notation for the general case. Suppose we have a symmetry group G where each element acts as an on-site unitary $u(g)$ as well as possibly implementing either time-reversal or spatial-inversion. One then can implement these elements on the MPS in terms of matrices $U(g)$ for $g \in G$ that satisfy [69]

$$U(g)\Lambda = \Lambda U(g), \qquad \sum_{b=0}^{N-1} u(g)_{a,b} \widetilde{\Gamma}_b = e^{i\varphi(g)} U(g) \Gamma_a U(g)^\dagger, \tag{39}$$

where Γ and Λ are the canonical decomposition of the MPS, and $\widetilde{\Gamma} = \Gamma$ for on-site global symmetries. When g implements lattice inversion, we have $\widetilde{\Gamma} = \Gamma^T$, while for the anti-unitary time-reversal $\widetilde{\Gamma} = \overline{\Gamma}$. Thus for our combined CPT symmetry, $\widetilde{\Gamma} = \Gamma^\dagger$.

The non-trivial symmetry fractionalisation for the ground state A_2 with even N follows from the $\mathbb{Z}_2 \times \mathbb{Z}_2^{\text{CPT}}$ subgroup of our D_{2N} symmetry. The $\mathbb{Z}_2$ symmetry from $X^{N/2}$ acting on a given site is implemented by matrices on the adjacent bonds by

$$\sum_{b=0}^{N-1} X_{a,b}^{N/2} \Gamma_b = Z^{N/2} \Gamma_a Z^{N/2}, \tag{40}$$

where the $X_{a,b}$ are the matrix elements of the operator X. For the $\mathbb{Z}_2^{\text{CPT}}$ symmetry,

$$\sum_{b=0}^{N-1} C_{ab} \left(\Gamma_b\right)^\dagger = e^{-2i\varphi} \left(e^{i\varphi} \sqrt{Z} V\right) \Gamma_j \left(e^{-i\varphi} V \sqrt{Z}^\dagger\right), \tag{41}$$

where C_{ab} are the matrix elements of the single-site charge-conjugation operator given in (21), and

$$\sqrt{Z} = \sum_{j=0}^{N-1} \omega^{j/2} |j\rangle \langle j|, \qquad V = V^\dagger = \sum_{j=0}^{N-1} |j\rangle \langle N-1-j|, \qquad e^{i\varphi} = \omega^{-\frac{N-1}{4}}, \tag{42}$$

where the bras and kets here are for the bond states. Note that this choice of V commutes with the Λ matrix, and for both generators we have used the freedom to fix the phases to make $U(g)^2 = 1$. (The overall phase $e^{-2i\varphi}$ does not enter into the representation matrices.)

Just as in the cluster model example, the non-trivial projective representation of $\mathbb{Z}_2 \times \mathbb{Z}_2^{\text{CPT}}$ on the bonds follows since the representation of these two generators does not commute:

$$\left(e^{i\varphi} \sqrt{Z} V\right) Z^{N/2} = -Z^{N/2} \left(e^{i\varphi} \sqrt{Z} V\right). \tag{43}$$

The two-dimensional irreducible projective representations of the symmetry group on the bonds requires the observed two-fold degeneracy in the entanglement spectrum. These properties are stable away from the fixed point, and cannot change without a bulk phase transition. Since this SPT order is protected by a subgroup $\mathbb{Z}_2 \times \mathbb{Z}_2^{\text{CPT}} \leq D_{2N}$, the SPT phase of A_2 remains stable under any perturbations preserving the subgroup, even if they break the full D_{2N}.

Despite not having SPT order, we still have symmetry fractionalisation in the ground state of A_2 for odd N. Our analysis of the $\mathbb{Z}_2^{\text{CPT}}$ generator in Eq. (41) applies for odd N. For all N, the full $\mathbb{Z}_N$ symmetry is implemented by

$$\sum_{b=0}^{N-1} X_{a,b}\, \Gamma_b = Z^{\dagger} \Gamma_a Z \,, \tag{44}$$

generalising (40). For $N = 2p + 1$ this action gives p irreducible two-dimensional linear representations of D_N, each of which acts on the basis $\{|b\rangle, |N-1-b\rangle\}$ as

$$r = \begin{pmatrix} \omega^b & 0 \\ 0 & \omega^{N-1-b} \end{pmatrix}, \qquad s = \begin{pmatrix} 0 & e^{i\varphi}\omega^{\frac{N-1-b}{2}} \\ e^{i\varphi}\omega^{\frac{b}{2}} & 0 \end{pmatrix}, \tag{45}$$

for $b = 0, \ldots, p-1$. A single one-dimensional representation acts on $|p\rangle$ as $r = \omega^p$ and $s = e^{i\varphi}\omega^{p/2}$.

The singlet occurs for the space with the smallest Schmidt value. All of the others, including the dominant ones, form two-dimensional irreducible representations of the non-Abelian D_{2N} symmetry group. This dimension of course cannot change continuously, so for small enough symmetry-preserving perturbations it cannot change without the system undergoing some sort of transition. This property therefore implies local stability of the phase. A phase with such behavior was dubbed a "representation SPT" (RSPT) [23]. Similar physics appears in other settings, including AKLT chains with even spin [73], quotient symmetry-protected topological order [6] and boundary-obstructed topological phases [74]. A transition out of an SPT phase must be a bulk one, as the representations are projective. The protection for the RSPT, however, is not as strong. A sufficiently large perturbation can change the dimension of the dominant Schmidt value without encountering a bulk phase transition, as shown in [25] for the model of [23].

Thus for odd N the ground state of A_2 can be deformed to that of A_0 without encountering a bulk phase transition or breaking the D_{2N} symmetry, as one expects in the absence of non-trivial SPT order. Before this transition, however, the phase exhibits SPT-like physical properties such as symmetry fractionalisation.

4.4 String order

String order parameters can be used to identify an SPT phase without explicitly calculating the symmetry fractionalisation considered above [69]. Indeed, we will use them to this effect in Section 5.3. In this section we identify the relevant string order parameter for the symetry group $D_{2N} = \mathbb{Z}_N \rtimes \mathbb{Z}_2^{\text{CPT}}$.

As above, there is a key distinction between even and odd N. Namely, the $\mathbb{Z}_N$ symmetry of the chiral-clock family possesses a $\mathbb{Z}_2$ subgroup for even N. We then can define a $\mathbb{Z}_2$ string operator using the "disorder" operator

$$\mu_k = \prod_{j=1}^{k-1} X_j^{N/2}, \qquad \left(\mu_k\right)^2 = 1 \,, \tag{46}$$

familiar from the Ising chain [75]. The limiting two-point function $\lim_{M,L\to\infty}\langle \mu_k \mu_{k+M}\rangle$ has a non-zero value only in the trivial phase. More generally we can dress μ_k with a local end-point

operator $\mathcal{O}_k$ (which is supported on some finite region to the right of site $k-1$). The key idea is that we will see long-range order in $\langle \mu_1 \mathcal{O}_1 \, \mu_k \mathcal{O}_k \rangle$ only when $\mathcal{O}_k$ has symmetry properties that are consistent with the SPT phase [69]. This notion can be generalised also to critical points and gapless phases [6,60,76],

In our particular D_{2N} setting, endpoint operators should have simple properties under conjugation by the CPT symmetry defined in Section 3.2. This symmetry is unusual since it combines an on-site unitary (charge conjugation), parity symmetry and anti-unitary time reversal. The ensuing complications require us to generalise the approach of [69] to such symmetries. In Appendix B we do so. Namely, we consider two-site Hermitian endpoint operators $\mathcal{O}_{k,k+1}$ satisfying

$$CP\mathcal{K} \, \mathcal{O}_{k,k+1} \, CP\mathcal{K} = s_c \, \mathcal{O}_{\hat{k},\hat{k}+1} X_{\hat{k}}^{N/2} X_{\hat{k}+1}^{N/2}, \qquad s_c = \pm 1. \tag{47}$$

There are two unusual aspects of this definition of the "charge" s_c, both due to applying the parity transformation P. First, the transformed operator is supported on the sites $\hat{k}, \hat{k}+1$, where $\widehat{k}$ is determined by which points are chosen to remain fixed under spatial inversion. Second, the charge is defined relative to multiplying by $X_{\hat{k}}^{N/2} X_{\hat{k}+1}^{N/2}$. The reason is that P inverts the string μ_k as well as the end-point operator, and the former needs to be multiplied by the global $\mathbb{Z}_2 = \mu_L$ to return it to a left-pointing string. Since we consider operators $\mu_k \mathcal{O}_k$, the extra factors can be absorbed into the end-point operator by multiplying it by $X_{\hat{k}}^{N/2} X_{\hat{k}+1}^{N/2}$. An MPS-based derivation allowing for a general end-point operator supported on more than two sites is given in Appendix B.

The charge s_c of the end-point of a string with long-range order reveals the SPT phase. In particular, for an end-point with $s_c = -1$, the asymptotic two-point function for $\mu_k \mathcal{O}_{k,k+1}$ is finite only in the SPT phase. (Recall there is only one non-trivial SPT phase for our symmetry group.) On the other hand, long-range order with $s_c = 1$ corresponds to the trivial phase.

The pivot procedure allows to find an end-point operator with $s_c = -1$ easily. Pivoting by the SPT entangler gives

$$U_1(\pi) X_k^{N/2} U_1(\pi) = \left(\sum_{m=1}^{N-1} \frac{1-(-1)^m}{1-\omega^m} Z_{k-1}^{-m} Z_k^m \right) X_k^{N/2} \left(\sum_{m=1}^{N-1} \frac{1-(-1)^m}{1-\omega^m} Z_k^{-m} Z_{k+1}^m \right), \tag{48}$$

where the dressing term squares to one (see Appendix A). The string therefore pivots to

$$\mu_k \mu_{k+M} \to \left(\sum_{m=1}^{N-1} \frac{1-(-1)^m}{1-\omega^m} Z_{k-1}^{-m} Z_k^m \right) \mu_k \mu_{k+M} \left(\sum_{m=1}^{N-1} \frac{1-(-1)^m}{1-\omega^m} Z_{k+M-1}^{-m} Z_{k+M}^m \right). \tag{49}$$

The end-point operators and the string overlap, and absorbing the ends of the former into the latter gives

$$\mathcal{O}_{k,k+1} = i X_k^{N/2} \left(\sum_{m=1}^{N-1} \frac{1-(-1)^m}{1-\omega^m} Z_k^{-m} Z_{k+1}^m \right) \implies \mu_k \mu_{k+M} \to \mu_k \mathcal{O}_{k-1,k} \, \mu_{k+M-1} \mathcal{O}_{k+M-1,k+M}. \tag{50}$$

The factor of i ensures $\mathcal{O}_{k,k+1}$ is Hermitian and that it transforms under CPT as in (47) with $s_c = -1$. For $N = 2$ it reduces to $i\sigma_k^x \sigma_k^z \sigma_{k+1}^z = \sigma_k^y \sigma_{k+1}^z$, the usual cluster-state end-point operator [46].

The ground state of A_0 is a product state and hence obviously in a trivial phase. Indeed, the disorder operator itself has long-range order:

$$\left\langle v_1^{(0)} v_2^{(0)} \cdots v_L^{(0)} \middle| \mu_k \mu_{k+M} \middle| v_1^{(0)} v_2^{(0)} \cdots v_L^{(0)} \right\rangle = 1. \tag{51}$$

We then exploit $\mu_{k+1} = \mu_k X_k^{N/2}$ and note that $X_k^{N/2}$ transforms under CPT as in (47) with $s_c = 1$. Thus our approach reproduces the triviality of the ground state of A_0.

Pivoting using (32) and (49) we then see immediately that (51) requires

$$\langle \psi_2 | \, \mathcal{O}_{k-1,k} \, \mu_{k+1} \, \mu_{k+M-1} \, \mathcal{O}_{k+M-1,k+M} \, | \psi_2 \rangle = 1 \,. \tag{52}$$

The ground state of A_2 therefore has long-range order for a string operator with end-point operator that obeys (47) with $s_c = -1$. We conclude that A_2 is in a non-trivial SPT phase, distinct from A_0, protected by $\mathbb{Z}_2 \times \mathbb{Z}_2^{\text{CPT}} \le D_{2N}$ for all even values of N. We thus recover the result found using symmetry fractionalisation in the preceding Section 4.3. The approach here emphasises the role of the $\mathbb{Z}_2$ symmetry present only at even N. Moreover, computing the string order via the operators in (52) provides a useful diagnostic tool for detecting a non-trivial phase away from the special points with an exact MPS ground state.

While the choice of end-point operator in Eq. (50) appears naturally by applying the SPT entangler to the disorder operator, there exist simpler end-point operators with the correct charge that may be useful in some situations:

$$\mathcal{O}'_{k,k+1} = \begin{cases} i X_k^{2n-1} Z_k^{2n-1} Z_{k+1}^{2n-1}, & N = 4n-2, \\ i X_k^{2k} \left(Z_k^{-1} Z_{k+1} + Z_k Z_{k+1}^{-1} \right), & N = 4n. \end{cases} \tag{53}$$

5 How the phases fit together

We have discussed in depth the three Hamiltonians A_0, A_1 and A_2 for the chiral-clock family. They respectively have no order, spontaneous symmetry breaking, and (R)SPT order. To probe the physics further, we combine them and analyse the Hamiltonian

$$H(\alpha, \beta, \gamma) = \alpha A_0 + \beta A_1 + \gamma A_2 \,. \tag{54}$$

The Hamiltonian $H(\alpha, \beta, \gamma)$ is integrable, as noted above in (18). However, deriving properties for $N > 2$ is rather difficult not only because of the interactions, but also due to the presence of level-crossing transitions in the ground state [35]. Nonetheless along certain lines we utilise and obtain analytic results. We also utilise density matrix renormalisation group (DMRG) [77, 78] numerics to understand the phase diagram for $N = 3$ and $N = 4$. We find that all these orderings extend away from these special solvable points, occupying regions of the phase diagram. For $N = 2$, the transitions between phases are direct, but for larger N intermediate gapless regions typically appear.

5.1 Special lines

Three special lines of couplings give useful insight into the phase diagram.

5.1.1 The Onsager-integrable chiral Potts line

The line $A_1 + \lambda A_0$ is the canonical Onsager-integrable chiral Potts chain. Much is known from extensive work some decades ago [17, 20, 22, 34, 35, 53, 54, 79, 80], but many puzzles remain. The main difficulty is that the lack of a $U(1)$ symmetry makes a traditional Bethe-ansatz analysis impractical. The ground-state phase diagram for $N = 3$ was analysed carefully in [35, 79, 81]. Along with the symmetry-breaking phase at $\lambda = 0$ and trivial phase for large λ, for $\lambda > 0$ there are two intermediate gapless phases for $\lambda_c < \lambda < 1$ and $1 < \lambda < 1/\lambda_c$, where $\lambda_c \simeq 0.901$ [35]. More recently, DMRG calculations at $\lambda = 1$ [82] found oscillations in the scaling of entanglement entropy for open boundaries. This behaviour is consistent with previous results for Lifshitz transitions [83]. The case of $\lambda < 0$ is equivalent, as follows from the results of Section 3.3.

Moreover, considering the energy of unit-charge excitations, long-range spin order occurs for all $\lambda < 1$ [35], including the intermediate gapless phase $\lambda_c < \lambda < 1$. We have not been able to observe the latter feature in our numerical studies below, and think that this long-range order in the gapless region is worth a deeper investigation. This intermediate region is further studied in Ref. [84], where scaling exponents for the order parameter are found; note that this gapless region is not described by a conformal field theory as the left- and right-moving excitations have different velocities [34,84,85]. These results can be summarised in the phase diagram

$$
\begin{array}{c}
\text{disorder} \qquad\qquad\qquad\qquad\qquad\qquad \text{disorder} \\[4pt]
\xrightarrow{\hspace{2.5cm}} \quad \overset{\text{ferromagnetic order}}{\xleftarrow{\hspace{3cm}}\hspace{0.1cm}\xrightarrow{\hspace{3cm}}} \quad \xleftarrow{\hspace{2.5cm}} \\[4pt]
\rule{13cm}{0.4pt} \quad \lambda\,. \\[-6pt]
-\lambda_c^{-1}\;-1\;\;-\lambda_c \qquad\qquad A_1 \qquad\qquad \lambda_c\;\;1\;\;\lambda_c^{-1}
\end{array}
\tag{55}
$$
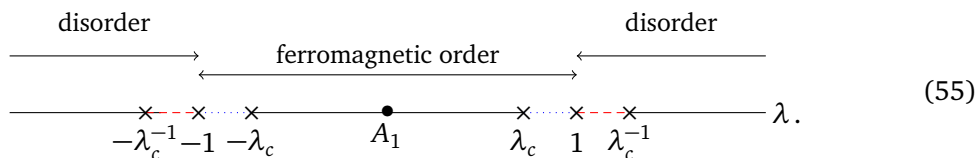
For $N > 3$ we are not aware of similar results for the phase diagram, although there are general formulae for structure of the spectrum [17,21,79,80] and both numerical and analytic studies of the spectrum for small system sizes [35,80]. For general N the ground state in the zero-momentum sector has a transition at $\lambda = 1$ [80,85]. This is not necessarily the ground state of the Hamiltonian because there may be a level crossing to a different momentum sector. In such a case, translation symmetry breaking [86] and/or an intermediate gapless phase or phases must occur. Our numerical studies described below in Section 5.3 indicate a similar structure for $N = 4$, including a first-order transition into an intermediate gapless phase.

A remarkable formula for the symmetry-breaking order parameter in the ferromagnetic phase was conjectured in [80] and proved (subject to certain analyticity assumptions) in [87, 88]. It is

$$
\lim_{M,L\to\infty} \left\langle Z_1^{-k} Z_M^k \right\rangle = (1 - \lambda^2)^{\frac{k(N-k)}{N^2}}, \qquad |\lambda| < \lambda_0\,,
\tag{56}
$$

where λ_0 indicates the first ground state phase transition we encounter beyond $\lambda = 0$ (moreover, for $N = 3$ we have a non-zero expectation for all $|\lambda| < 1$, based on the analysis of Ref. [35]). Duality yields

$$
\lim_{M,L\to\infty} \left\langle \prod_{j=1}^{M} X_j^k \right\rangle = (1 - \lambda^{-2})^{\frac{k(N-k)}{N^2}}, \qquad |\lambda| > \lambda_0^{-1}\,.
\tag{57}
$$

The (trivial) string-order parameter thus takes the N-independent value

$$
\lim_{M,L\to\infty} \left\langle \mu_1 \mu_M \right\rangle = (1 - \lambda^{-2})^{\frac{1}{4}}, \qquad |\lambda| > \lambda_0^{-1}\,.
\tag{58}
$$

5.1.2 The line $A_1 + \lambda A_2$

Pivoting the preceding Hamiltonian with $U_1(\pi)$ means that the Hamiltonian $A_1 + \lambda A_2$ is unitarily equivalent. The transitions must therefore occur at the same values of λ_c. However, the physical interpretation of the phases is rather different. We saw already that A_2 possesses (R)SPT order. Transforming the trivial string order from (58) immediately shows the SPT order exists away from A_2. Namely, using (49) yields exact topological string order at even N:

$$
\lim_{M,L\to\infty} \left\langle \mu_1 \mathcal{O}_{1,2}\, \mu_M \mathcal{O}_{M,M+1} \right\rangle = (1 - \lambda^{-2})^{\frac{1}{4}}, \qquad |\lambda| > \lambda_0^{-1}\,.
\tag{59}
$$

The SPT order therefore persists at least until $\lambda = \lambda_c^{-1}$ (as it must on general stability grounds), and likely all the way until $\lambda = 1$, as summarized in the diagram

$$
\begin{array}{c}
\text{(R)SPT} \qquad\qquad\qquad\qquad\qquad\qquad\qquad \text{(R)SPT} \\
\longrightarrow \qquad\qquad\qquad \text{ferromagnetic order} \qquad\qquad \longleftarrow \\
\underset{-\lambda_c^{-1}\ -1\ -\lambda_c}{\times\!-\!\!-\!\times\cdots\times} \qquad \underset{A_1}{\bullet} \qquad \underset{\lambda_c\quad 1\quad \lambda_c^{-1}}{\times\cdots\times\!-\!\!-\!\times} \qquad \lambda \,.
\end{array}
\tag{60}
$$
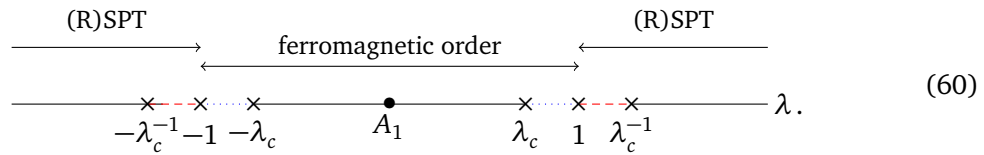
Subtleties with SPT physics arise in gapless models [6], but resolving them requires a deeper understanding of the nature of the gapless phase realised here. Moreover, we cannot prove that the RSPT phase at odd N persists, even in the gapped region, but we expect that the dominant Schmidt value remains doubly degenerate throughout. Below we give numerics in support of this contention.

5.1.3 The $U(1)$ line and the exact ferromagnetic ground state

Setting $\alpha = \gamma$ in (54) yields a rather special line of Hamiltonians. Namely, it follows immediately from (4) that A_1 commutes with $A_0 + A_2$:

$$
\left[A_1, \alpha A_0 + \beta A_1 + \alpha A_2\right] = 0 \,.
\tag{61}
$$

Since NA_1 has integer eigenvalues, it generates a $U(1)$ symmetry along this line. An explicit expression for the KW dual Hamiltonian in terms of the usual $SU(2)$ operators $S^\pm, S^z$ can be found in [38].

This $U(1)$ symmetry allows the coordinate Bethe ansatz to be used, as described in depth in [38] for a closely related $U(1)$-invariant model. Acting with the Onsager generators turns out to correspond to adding or removing "exact strings" within the Bethe ansatz. A conjecture was made there that the ground state of the model $A_1 + A_{-1}$ (the dual of $A_0 + A_2$) is comprised solely of such exact strings. Our detailed calculations show however that this property holds true only for $L \leq 12$. Thus the analysis, while tractable, is still rather difficult. We defer a full accounting to a separate paper [37].

However, the $U(1)$ symmetry does result in an exact ground state over a range of α/β when $\alpha = \gamma$. When $H = A_1$, the N ground states are given by all spins equal in the Z-basis, as shown in (29). Each such state is annihilated by $A_0 + A_2$. Moving away from A_1 by allowing $\alpha = \gamma \neq 0$, the different ground states do not mix in perturbation theory until order L, and the exact ferromagnetic ground states persist until the $\alpha = \gamma$ is of order β. For $N = 2$, this transition occurs exactly at $\alpha = \gamma = \beta/2$. This value is recovered by a simple first-order perturbation theory in the one-particle sector [89], giving a transition at $\alpha/\beta = \gamma/\beta = \sin(\pi/N)/2$. For $N = 3, 4$, and for $\alpha = \gamma = 1/2$, this predicts $\beta \simeq 1.15, 1.41$ respectively. These values are consistent with the numerics in Fig. 4, though the transition appears to occur for a larger value of β in the $N = 4$ case.

5.2 Phase diagram for $N = 2$

We first consider the full phase diagram in the $N = 2$ free-fermion case, where it is known exactly. This case is KW dual to the usual quantum XY model [90], and so phase transitions occur at the same places. The results are displayed in Fig. 3(a), with the trivial, SPT and ferromagnetic phases readily apparent.

The line from Section 5.1.1 with $\gamma = 0$ corresponds at $N = 2$ to the usual transverse-field Ising model, while pivoting with A_1 yields the line with $\alpha = 0$ described in (5.1.2). Onsager's results show that these models have Ising critical points at $\alpha = \beta$ and $\gamma = \beta$ respectively.

(a) $N = 2$. (b) $N = 3$. (c) $N = 4$.
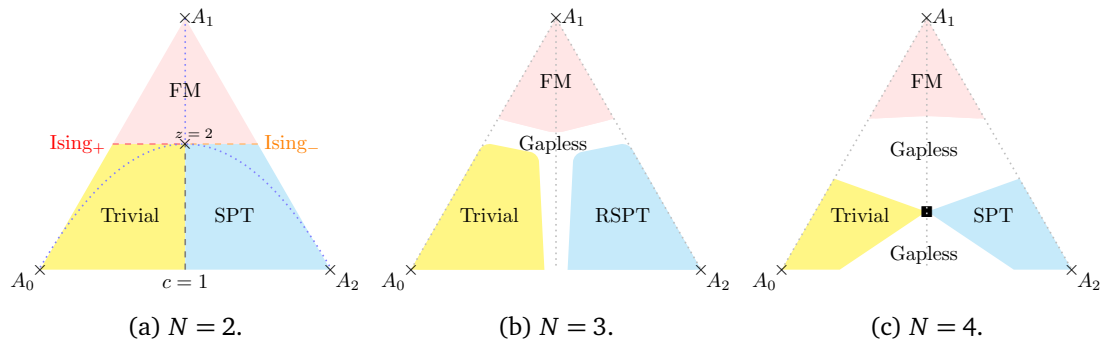
Figure 3: Schematic phase diagrams for $N = 2, 3, 4$ for the Hamiltonian $H(\alpha, \beta, \gamma)$ parameterised as $\alpha + \beta + \gamma = 1$. FM indicates the ferromagnetic phase. The $N = 2$ phase diagram is known exactly and features direct transitions. An exact MPS ground state occurs on the dotted line. For $N = 3, 4$ the transitions typically spread out into gapless regions. Within the achieved numerical resolution, we cannot ascertain whether we have a narrow gapless region or a direct transition between the trivial and SPT phases for a certain range along the $\alpha = \gamma$ line for $N = 4$ (indicated by ■). The grey dotted lines are discussed in Section 5.1.

The latter criticality is enriched by $\mathbb{Z}_2 \times \mathbb{Z}_2^{\mathrm{CPT}}$ [6], as confirmed by our analysis of the string order in Section 4.4 for all even N. Since the disorder operator has charge $s_c = 1$ and $s_c = -1$ under CPT for trivial and SPT phases respectively, the corresponding critical points are labelled Ising$_\pm$.

The transition between the trivial and SPT phases along the $\beta = 0$ line occurs at the $U(1)$ invariant value $\alpha = \gamma$ for $N = 2$. Its continuum limit is described by a single free-boson field theory, a conformal field theory with central charge $c = 1$. The type of criticality is invariant (and the $c = 1$ remains at the free-fermion radius) up to the multicritical point at $\alpha = \gamma = \beta/2$. The multicritical point has dynamical critical exponent $z = 2$, and the charge of the disorder operator changes sign along the Ising CFT line here. This point also has an exact MPS ground state, as does the model along the dotted line [91–94] with couplings $\alpha = (1 - \lambda)^2, \beta = 2\lambda(1 - \lambda), \gamma = \lambda^2$. This line is dual to the disorder line in the XY model [95–97].

5.3 Phase diagram for $N = 3, 4$

To determine the full phase diagrams $H(\alpha, \beta, \gamma)$ for $N = 3, 4$, we need to distinguish the three phases: trivial, symmetry breaking and (R)SPT dominated by A_0, A_1, A_2 respectively. Here we use the density matrix renormalization group (DMRG) [98] to go beyond the above analytic results. All following numerical calculations were performed using the ITensor library [77,78] for finite systems with open boundary conditions. We summarise our results in Fig. 3, showing that the critical lines seen in the $N = 2$ case broaden out to gapless regions. A key result is that the RSPT order at $N = 3$ remains throughout a region.

We use a variety of probes to determine the phase diagrams. For example, we give results from entanglement entropy in Fig. 4. The probes are discussed in each of the following subsections.

5.3.1 Local and string order parameters

A non-vanishing value of the two-point correlation function

$$\mathcal{O}_Z = \left| \left\langle Z_j Z_k^{-1} \right\rangle \right| \tag{62}$$

(a) $N = 3$.   (b) $N = 4$.
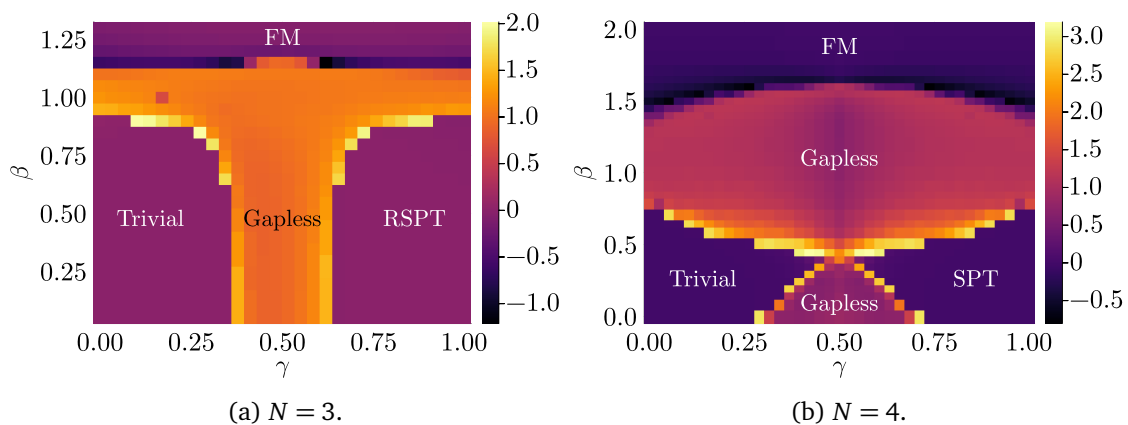
Figure 4: The effective central charge c for $H(\alpha, \beta, \gamma)$ with $\alpha = 1 - \gamma$ for (a) $N = 3$ and $L = 100$, (b) $N = 4$ and $L = 40$. The value is extracted by fitting the entanglement entropy to the CFT formula Eq. (66). A zero value indicates an area-law ground state. Values of c at the boundary of the gapless region are not meaningful. A unitary transformation relates Hamiltonians with γ and $1 - \gamma$, and so the data for $N = 4$ for $\gamma > 0.5$ is that for $\gamma \leq 0.5$.

at large $|j - k|$ indicates ferromagnetic order. As seen in Fig. 5(b) and (d), such order occurs at large β where A_1 dominates the Hamiltonian.

The string operators discussed in Section 4.4 provide a convenient way to distinguish the SPT phase and trivial phases at even N. The trivial phase at even N is detected by the two-point function of disorder operators, namely

$$\mathcal{S}_0 = |\langle \mu_j \mu_k \rangle|. \tag{63}$$

The SPT phase, on the other hand, is detected by pivoting Eq. (63) using the SPT entangler as discussed in Section 4.4. For $N = 4$, we show in Appendix B.2, that the relevant string order (50) takes on the form

$$\mathcal{S}_1 = \left| \left\langle \tfrac{i}{2} \left(S^{-1,-1} - S_{1,1} \right) + S^{-1,1} \right\rangle \right|, \qquad S^{a,b} \equiv Z_{j-1}^a Z_j^{-a} \mu_j \mu_{k+1} Z_k^b Z_{k+1}^{-b}. \tag{64}$$

Non-vanishing values of these two-point functions (Equations (63) and (64) for large values of $|j - k|$) are good order parameters for the trivial and SPT phases respectively. We plot these values in Fig. 5(c,d) for $j = L/4$ and $k = 3L/4$, indicating the presence of these phases when A_0 and A_2 respectively dominate.

5.3.2 Entanglement spectrum

The bipartite entanglement spectrum of the ground states provides a useful probe for detecting the SPT and RSPT phases. The values are Λ_α^2, where the Λ_α are the usual Schmidt coefficients of the ground state [24, 69, 71]. The entanglement spectrum of SPT phases is characterized by the presence of robust degeneracies for all Λ_α and the total absence of non-degenerate values, shown in Fig. 6(b). The trivial and RSPT phases contain non-degenerate entanglement levels along with degenerate ones. These two phases are distinguished by the nature of the dominant Schmidt value. In the trivial phase it is unique, whereas in the RSPT phase it is degenerate, as shown in Fig. 6(a). These results confirm the stability of our analytic results in Section 4.2 away from the fixed point model A_2 for both even and odd N. By tracking the gap $\Delta_\Lambda = \Lambda_1^2 - \Lambda_2^2$ between the leading entanglement values, we can distinguish the trivial from the RSPT. As apparent in Fig. 5, Δ_Λ vanishes for the former but not the latter.
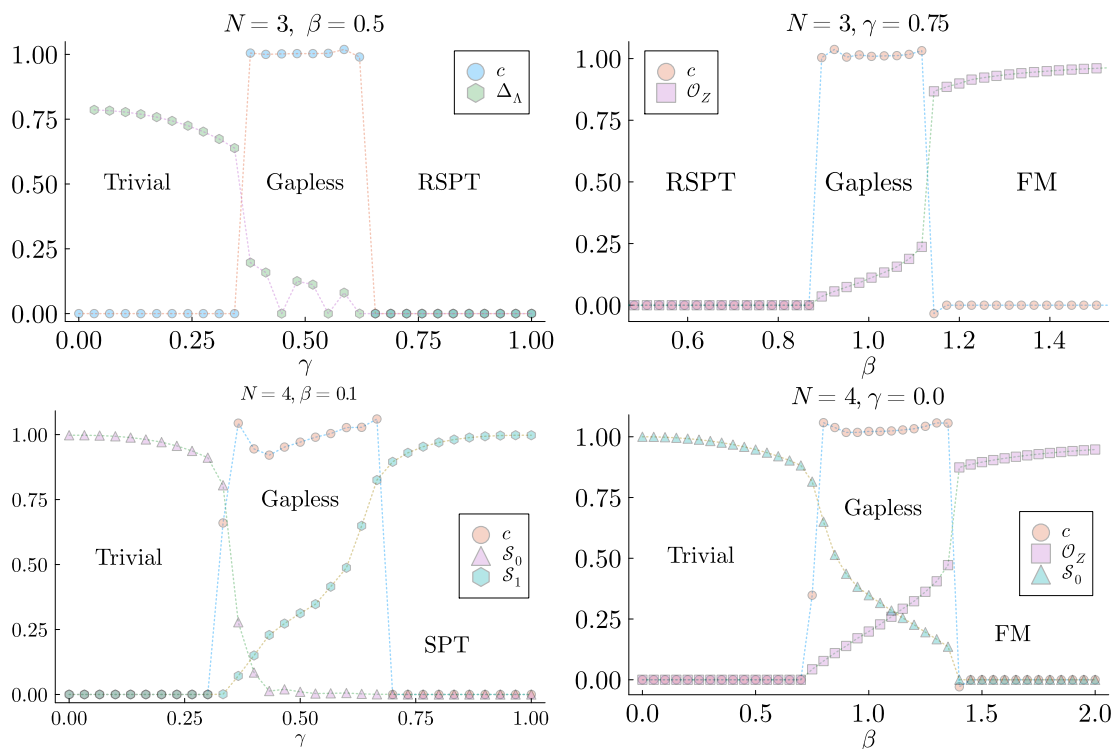
Figure 5: DMRG calculations for the $N = 3$ (a,b) and $N = 4$ (c,d) versions of the Hamiltonian (54) with $\alpha = 1 - \gamma$ and with system sizes $L = 200$ and $L = 100$ respectively. $\mathcal{O}_Z$ is the local order parameter shown in Eq. (62), $\mathcal{S}_0$ and $\mathcal{S}_1$ are the trivial and non-trivial string order parameters defined in Eqs. (63) and (64) respectively, while c comes from fitting the entanglement entropy to Eq. (66). The Schmidt value Λ_α comes from the mid-chain bipartite Schmidt decomposition of the ground state, and the difference between the largest two values $\Delta_\Lambda = \Lambda_1^2 - \Lambda_2^2$. Dotted lines connecting data points are provided as a guide to the eye.

In a general context, the entanglement spectrum is known to be an indirect probe of the edge modes in a topological phase [99]. Similarly, the degeneracy of the largest entanglement levels in the RSPT is expected to result in parametrically stable edge modes, despite lacking in topological protection [23,25,30,31]. A simple pivoting calculation reveals that the fixed-point A_2 with open boundaries has N^2 ground states. However, the relation between entanglement spectrum and edge modes is known to break down when parity symmetry is involved [73], and indeed one can find symmetric boundary terms that gap out these edge modes for any non-zero coupling. Thus, the entanglement spectrum is the most relevant probe of the (R)SPT physics.

5.3.3 Entanglement entropy

The von Neumann entanglement entropy provides a good way to distinguish the gapless phases from the gapped ones. It is defined as

$$S(l_A) = -\text{tr}(\rho_A \log \rho_A), \tag{65}$$

where ρ_A is the reduced density matrix with support on the Hilbert space A, taken to be a contiguous interval length l on the chain. For ground states of one-dimensional gapped phases, $S(l) \sim \text{const.}$, an area law. Critical gapless phases that are described by a 1+1-dimensional
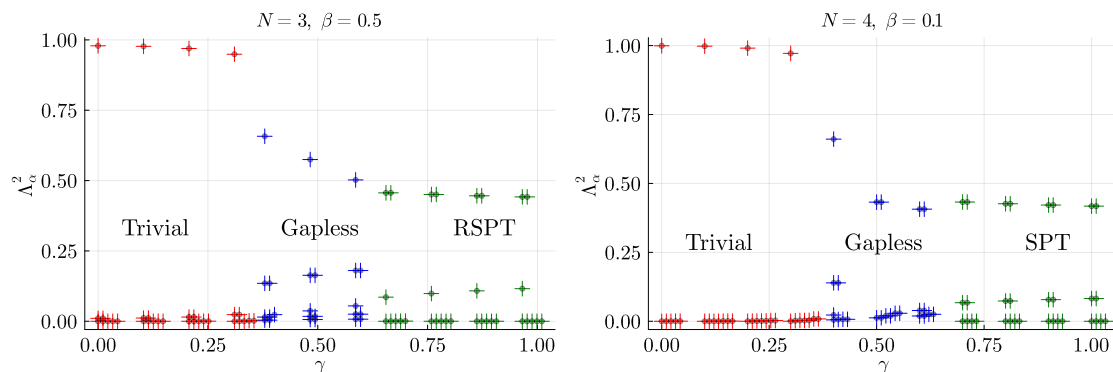
Figure 6: The entanglement spectrum for the ground state of (54) with $\alpha = 1 - \gamma$ and system size $L = 200$. All levels are doubly degenerate in the SPT phase, while both degenerate and non-degenerate values occur in the RSPT and trivial phases. The latter two phases are distinguished by the dominant entanglement level, which is unique for the trivial phase but degenerate for the RSPT.

conformal field theory obey a universal form [100] of entanglement scaling in the large-L limit. For a finite system of size L with open boundary conditions,

$$S(l) = \frac{c}{6} \log\left(\frac{L}{\pi} \sin\left(\frac{\pi l}{L}\right)\right) + \text{const.}, \tag{66}$$

where c is the central charge that characterizes the CFT. Entanglement entropy obeying the form Eq. (66) thus indicates gapless behaviour, with $c \neq 0$ providing a measure of entanglement.

As seen in Fig. 5, this fit can be used effectively to distinguish the gapless phases from the surrounding gapped ones. We apply this procedure to locate the gapless regions in Figs. 3 and 4. We find that the data fits well to Eq. (66) with $c = 1$, as shown in Fig. 7, suggesting that the gapless states are described by a compact boson CFT or its orbifold [101]. However, as shown in Fig. 7(b), we observe oscillations in certain ranges of parameter values. As discussed in Section 5.1.1, these are also consistent with Lifshitz transitions [83] and have been observed in numerical investigations of similar models [82]. Similar results are seen for the gapless states appearing in the phase diagram of the $N = 4$ Hamiltonian. The precise nature of the gapless states appearing in our phase diagrams is an interesting question, which we leave for upcoming work.

6 Outlook

In this paper we showed how the Onsager algebra naturally gives rise to a pivot procedure useful for constructing SPT phases. We applied this result to a family of N-state chiral clock Hamiltonians constructed with this algebra. We found an SPT phase for even N and an RSPT phase for odd N, protected by the dihedral group D_{2N} comprised of the clock and CPT symmetries.

We analysed in depth the Hamiltonian A_2, the N-state analog of the cluster-model SPT. We found an analytic expression for the entanglement spectrum in its MPS ground state, and showed it has dominant, degenerate Schmidt values in the entanglement spectrum. For even N, the ground state has non-trivial SPT order characterised by a projective representation of D_{2N} on the bond Hilbert space. We showed that this SPT phase can be detected by a string order parameter with an end-point charged under $\mathbb{Z}_2^{\text{CPT}}$. For odd N, however, every Schmidt
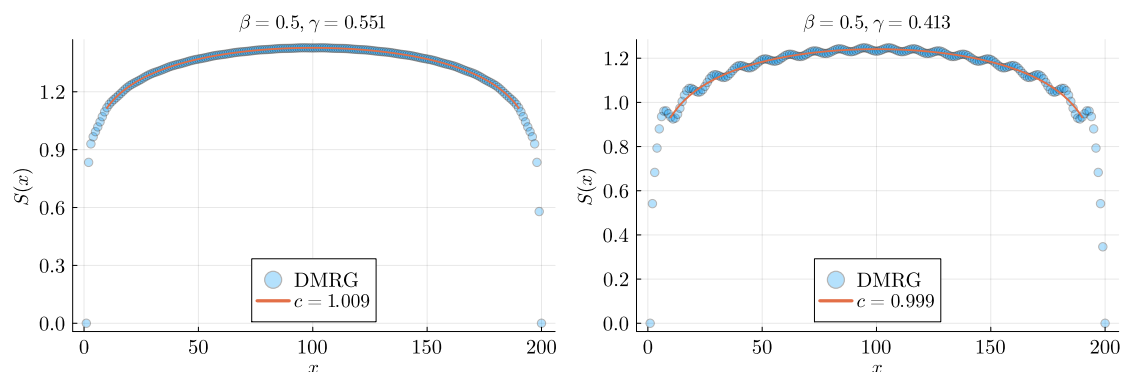
Figure 7: Von Neumann entanglement entropy computed for representative gapless ground states of the $N = 3$ Hamiltonian (54) with $\alpha = 1 - \gamma$ and system size $L = 200$, (datapoints) compared with the best fit to the CFT formula Eq. (66). Both have a best fit of $c \approx 1$ (solid line), with oscillations observed for some parameters (b) but absent for others (a).

value of the ground state of A_2 is degenerate apart from the smallest one. This entanglement spectrum is inconsistent with any projective representation on the bonds, and thus corresponds to a trivial SPT phase (for any protecting symmetry group). However, the system has dominant degenerate Schmidt values corresponding to higher-dimensional irreducible representations of D_{2N} and we conclude that A_2 represents an RSPT phase for D_{2N}.

The phase diagram interpolating between A_0, A_1 and A_2 is rich, and based on analytic and numerical results we conjectured its form for $N = 3, 4$. For even N the three fixed-point Hamiltonians represent distinct phases of matter, and thus are separated by bulk transitions. We demonstrated that the RSPT phase in the case $N = 3$ does extend away from the fixed-point A_2 by numerically calculating the entanglement gap using DMRG [77, 78]. We moreover see a critical phase separating this RSPT from the trivial phase, which is "unnecessary" from the SPT point of view [28–32].

A key topic for future work is to better understand the phase diagrams outlined in Section 5.3. Particularly interesting would be substructure within the gapless regions, and possible symmetry enrichment. Indeed, our numerical investigations leave open the possibility that the $N = 4$ phase diagram contains two separate gapless regions meeting at a direct transition between the trivial and SPT phases [31, 76]. In a companion work, we consider the $U(1)$ invariant line $A_0 + A_2 + hA_1$, along with the KW dual $A_1 + A_{-1} + hA_0$ (where the $U(1)$ symmetry is on-site); note that this line includes the possible direct transition. This symmetry lends itself to a coordinate Bethe Ansatz approach. We have left the wider phase diagram for the chiral clock family $H = \sum t_\alpha A_\alpha$ unexplored. While there is only one non-trivial SPT phase for our symmetry group, we may see combined symmetry-breaking and SPT physics in the higher Hamiltonians [5]. Identifying the gapless regions in this larger phase diagram would also be interesting.

Our results are not restricted to the Onsager-integrable chiral-clock family we have studied. The D_{2N} symmetry identified here occurs in more general chiral clock models. The $\mathbb{Z}_2^{\mathrm{CPT}}$ symmetry takes, for example, $\gamma X_n \to \bar{\gamma} X_n^\dagger$. It follows that any Hermitian $H = \sum_j \sum_{m=1}^{N-1} \left(\gamma_m h_{2j-1}^m + \delta_m h_{2j}^m \right)$ has this symmetry, along with the standard clock symmetry. Hence, the SPT phase (and possibly the RSPT phase) will extend into the wider phase diagram of the chiral clock models [82].

A natural next step is to look for SPT physics and interesting phase diagrams in other families of spin chains that generate an Onsager algebra, such as those in Refs. [102–104]. Further examples can be found in the setting of generalised Onsager algebras; there we have mul-

tiple generators each satisfying a mutual Dolan-Grady relation [105, 106]. A fundamentally different model to those considered in this paper is the "free fermions in disguise" Hamiltonian [107], which can be written as a sum of terms satisfying a generalised Onsager algebra [106]. It would be most interesting to uncover a new family in this class.

One final outstanding question is to find which subspace of the phase diagram has an exact MPS ground state, generalising the line in Fig. 3(a). The solution to this problem for $N = 2$ utilises imaginary time evolution with fixed-point Hamiltonians [93], and the Onsager algebra may allow for a generalisation of this approach.

Acknowledgments

We are grateful to Murray Batchelor, Yuchi He, Barry McCoy, Max McGinley, Yuan Miao and Ryan Thorngren for helpful discussions and correspondence. We also thank Ruben Verresen and Nathanan Tantivasadakarn for sharing their insights and their related results [25].

Funding information This work was supported by the European Research Council under the European Union Horizon 2020 Research and Innovation Programme, Grant Agreement No. 804213-TMCS (A.P), and by EPSRC grant EP/X030881/1 (P.F.). Preliminary work was completed while N.G.J. held a Heilbronn Research Fellowship at the Mathematical Institute, University of Oxford.

A   Derivation of the Hamiltonian A_2

In this appendix we derive the closed-form expression for A_2 given in the main text (17). There are two paths one can take

$$A_2 = U_1 A_0 U_1^\dagger, \qquad \text{and} \qquad A_2 = A_0 + \frac{1}{8}\big[A_1,[A_0,A_1]\big]. \tag{A.1}$$

We give both the pivot and commutator approaches for the Kramers-Wannier dual operator A_{-1}, and then connect the two to reach our preferred representation for A_2.

A.1   Pivoting A_1 with A_0 to find A_{-1}

We first use the pivot procedure to find $A_{-1} = U_0(\pi) A_1 U_0(\pi)^\dagger$. We can write $U_0(\pi)$ as a product of single-site terms, so that its action on the single-site operator Z is

$$\widehat{Z} = e^{i\frac{\pi}{N}\sum_{m=1}^{N-1}\alpha_m X^m} Z\, e^{-i\frac{\pi}{N}\sum_{m=1}^{N-1}\alpha_m X^m}. \tag{A.2}$$

In the X basis, $X = \sum_a \omega^{-a}\left|v^{(a)}\right\rangle\left\langle v^{(a)}\right|$ and $Z = \sum_a \left|v^{(a-1)}\right\rangle\left\langle v^{(a)}\right|$, so

$$
\begin{aligned}
\widehat{Z} &= \sum_{a=0}^{N-1} e^{i\frac{\pi}{N}\sum_{m=1}^{N-1}(\alpha_m \omega^{-m(a-1)} - \alpha_m \omega^{-ma})}\left|v^{(a-1)}\right\rangle\left\langle v^{(a)}\right| \\
&= e^{i\frac{\pi}{N}}\sum_{a=0}^{N-1}(-1)^{\delta_{a,0}}\left|v^{(a-1)}\right\rangle\left\langle v^{(a)}\right| = e^{i\pi/N} Z \hat{\Phi}^{(0)},
\end{aligned}
\tag{A.3}
$$

where

$$\widehat{\Phi}_j^{(r)} \equiv \sum_a (-1)^{\delta_{r-a,0}}\left|v_j^{(a)}\right\rangle\left\langle v_j^{(a)}\right|, \qquad \widehat{\Phi}_j^{(r)} Z_j = Z_j \widehat{\Phi}_j^{(r+1)}. \tag{A.4}$$

Obviously, $\left(\widehat{\Phi}_j^{(r)}\right)^2 = 1$ so that

$$U_0(\pi)Z_j^k U_0(\pi)^\dagger = \omega^{k/2} Z_j^k \prod_{r=0}^{k-1} \widehat{\Phi}_j^{(r)}, \tag{A.5}$$

$$A_{-1} = U_0(\pi)A_1 U_0(\pi)^\dagger = -\frac{4}{N}\sum_{j=1}^{L}\sum_{m=1}^{N-1}\alpha_m\left(\prod_{r=0}^{m-1}\widehat{\Phi}_j^{(r)}\right)Z_j^{-m}Z_{j+1}^m\left(\prod_{r=0}^{m-1}\widehat{\Phi}_{j+1}^{(r)}\right). \tag{A.6}$$

A.2 Pivoting A_0 with A_1 to find A_2

One can find A_2 by exchanging A_0 and A_1 in the preceding pivot, as follows from (11). The calculation then proceeds identically if one utilises the operators h_k from (15). One then finds

$$A_2 = -\frac{4}{N}\sum_{j=1}^{L}\sum_{m=1}^{N-1}\alpha_m\left(\prod_{r=0}^{m-1}\Phi_{j-1,j}^{(r)}\right)X_j^m\left(\prod_{r=0}^{m-1}\Phi_{j,j+1}^{(r)}\right), \tag{A.7}$$

where

$$\Phi_{j,j+1}^{(r)} = \sum_{a_1,a_2}(-1)^{\delta_{a_2-a_1+r,0}}\,|a_1\rangle_j\,\langle a_1|_j\,|a_2\rangle_{j+1}\,\langle a_2|_{j+1}. \tag{A.8}$$

We show in Appendix A.4 how to rewrite this product of signs in terms of Z_j operators.

A byproduct of this calculation is that $U_1(\pi)X_j U_1(\pi)^\dagger = \Phi_{j-1,j}^{(0)}X_j\Phi_{j,j+1}^{(0)}$. Since X acts as a shift in the Z-basis, we have

$$\Phi_{j,j+1}^{(r)}X_j = X_j\Phi_{j,j+1}^{(r+1)}, \qquad \Phi_{j,j+1}^{(r)}X_{j+1} = X_{j+1}\Phi_{j,j+1}^{(r-1)}, \tag{A.9}$$

yielding (48) and the resulting transformed string operator.

A.3 Commutator calculation

In this section we derive a closed-form expression for A_{-1} using commutation relations directly.

Using the definitions of A_0 and A_1 from (15,16) gives

$$[A_0,A_1] = \left(\frac{4}{N}\right)^2\sum_{j=1}^{L}\sum_{a,\hat{a}=1}^{N-1}\alpha_a\alpha_{\hat{a}}(1-\omega^{a\hat{a}})\left(h_{2j-1}^a h_{2j}^{\hat{a}} - h_{2j}^{\hat{a}} h_{2j+1}^a\right). \tag{A.10}$$

A useful identity proved below is

$$\sum_{a,b=1}^{N-1}\alpha_{a,\hat{a}}\alpha_{b,\hat{a}}h_{2j-1}^{a+b} = \hat{a}(N-\hat{a}) + (N-2\hat{a})\sum_{s=1}^{N-1}\alpha_{s,\hat{a}}h_{2j-1}^{s}, \tag{A.11}$$

where we define $\alpha_{a,\hat{a}} = \alpha_a(1-\omega^{a\hat{a}})$. Commuting A_0 with (A.10) and using this identity yields

$$[A_0,[A_0,A_1]] = -\left(\frac{4}{N}\right)^3\sum_{j=1}^{L}\left(-2\sum_{a,\hat{a},b=1}^{N-1}\alpha_{a,\hat{a}}\alpha_{\hat{a}}\alpha_{b,\hat{a}}h_{2j-1}^a h_{2j}^{\hat{a}} h_{2j+1}^b\right. \tag{A.12}$$

$$\left. + \sum_{a,\hat{a}=1}^{N-1}\alpha_{a,\hat{a}}\alpha_{\hat{a}}(N-2\hat{a})\left(h_{2j-1}^a h_{2j}^{\hat{a}} + h_{2j}^{\hat{a}} h_{2j+1}^a\right) + 2\sum_{\hat{a}=1}^{N-1}\hat{a}(N-\hat{a})\alpha_{\hat{a}}h_{2j}^{\hat{a}}\right).$$

The Onsager algebra requires

$$A_{-1} = A_1 - \frac{1}{8}\Big[A_0,[A_0,A_1]\Big], \tag{A.13}$$

so that

$$A_{-1} = -\frac{4}{N^3}\sum_{j=1}^{L}\left(4\sum_{a,\hat{a},b=1}^{N-1}\alpha_a\alpha_{\hat{a}}\alpha_b(1-\omega^{a\hat{a}})(1-\omega^{b\hat{a}})h_{2j-1}^a h_{2j}^{\hat{a}} h_{2j+1}^b\right.$$

$$\left.-2\sum_{a,\hat{a}=1}^{N-1}\alpha_a\alpha_{\hat{a}}(N-2\hat{a})(1-\omega^{a\hat{a}})\left(h_{2j-1}^a h_{2j}^{\hat{a}}+h_{2j}^{\hat{a}} h_{2j+1}^a\right)+\sum_{\hat{a}=1}^{N-1}(N-2\hat{a})^2\alpha_{\hat{a}}h_{2j}^{\hat{a}}\right)$$

$$= -\frac{4}{N}\sum_{j}\sum_{\hat{a}=1}^{N-1}\alpha_{\hat{a}}\left(1-\frac{2\hat{a}}{N}-\frac{2}{N}\sum_{a=1}^{N-1}\alpha_{a,\hat{a}}h_{2j-1}^a\right)h_{2j}^{\hat{a}}\left(1-\frac{2\hat{a}}{N}-\frac{2}{N}\sum_{b=1}^{N-1}\alpha_{b,\hat{a}}h_{2j+1}^b\right). \tag{A.14}$$

Finally, note that taking (A.12) and doing another commutator gives the Dolan-Grady relation:

$$\left[A_0,\left[A_0,[A_0,A_1]\right]\right] = \left(\frac{4}{N}\right)^4\left(2\hat{a}(N-\hat{a})+(N-2\hat{a})^2+2\hat{a}(N-\hat{a})\right)$$

$$\times\sum_{j=1}^{L}\sum_{a,\hat{a}=1}^{N-1}\alpha_{a,\hat{a}}\alpha_{\hat{a}}\left(h_{2j-1}^a h_{2j}^{\hat{a}}-h_{2j}^{\hat{a}} h_{2j+1}^a\right)$$

$$= 16\left[A_0,A_1\right]. \tag{A.15}$$

A.3.1 Proof of (A.11)

Consider the following action:

$$\sum_{a,b=0}^{N-1}\omega^{ka}\omega^{lb}X^{a+b}\left|v^{(j)}\right\rangle = \sum_{a,b=0}^{N-1}\omega^{ka+lb-ja-jb}\left|v^{(j)}\right\rangle = N^2\delta_{k,j}\delta_{l,j}\left|v^{(j)}\right\rangle. \tag{A.16}$$

Using geometric series and the vanishing of the previous double sum for $k\neq l$ yields

$$\sum_{a,b=1}^{N-1}\alpha_{a,\hat{a}}\alpha_{b,\hat{a}}X^{a+b} = \sum_{k,l=0}^{\hat{a}-1}\sum_{a,b=1}^{N-1}\omega^{ka+lb}X^{a+b} = \sum_{k,l=0}^{\hat{a}-1}\sum_{a,b=0}^{N-1}\omega^{ka+lb}X^{a+b}-2\hat{a}\sum_{a=1}^{N-1}\sum_{k=0}^{\hat{a}-1}\omega^{ka}X^a-\hat{a}^2$$

$$= \hat{a}(N-\hat{a})+(N-2\hat{a})\sum_{a=1}^{N-1}\sum_{k=0}^{\hat{a}-1}\omega^{ka}X^a. \tag{A.17}$$

A.4 Connecting the two approaches

In this section we show that the formula for A_{-1} written in terms of $\widehat{\Phi}_n$ is the same as the expression (A.14). In particular, we show:

$$\left(\prod_{r=0}^{m-1}\widehat{\Phi}_j^{(r)}\right) = \widehat{S}_j^{(m)} \equiv 1-\frac{2m}{N}-\frac{2}{N}\sum_{m'=1}^{N-1}\frac{1}{1-\omega^{m'}}(1-\omega^{mm'})X_j^{m'}. \tag{A.18}$$

First, notice that the identity (A.11) yields

$$\left(S_j^{(m)}\right)^2 = \left(\widehat{S}_j^{(m)}\right)^2 = 1, \tag{A.19}$$

for any m, j. Thus the dressing terms are operators squaring to a constant. Indeed,

$$\left(1-\frac{2}{N}\sum_{m'=0}^{N-1}\omega^{(r-a)m'}\right)\left|v_j^{(a)}\right\rangle = (1-2\delta_{r-a,0})\left|v_j^{(a)}\right\rangle = (-1)^{\delta_{r-a,0}}\left|v_j^{(a)}\right\rangle = \widehat{\Phi}_j^{(r)}\left|v_j^{(a)}\right\rangle. \tag{A.20}$$
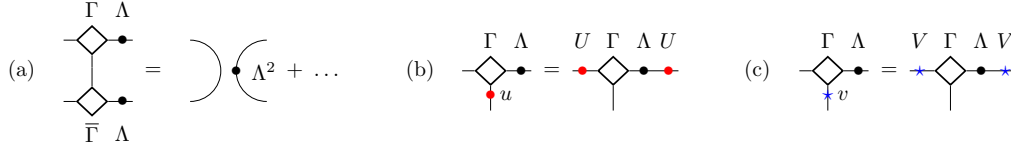
Figure 8: Graphical identities for an MPS tensor with $\mathbb{Z}_2 \times \mathbb{Z}_2$ symmetry generated by $\prod_k u_k$ and $\prod_k v_k$: (a) the transfer matrix in canonical form (b) symmetry fractionalisation of u (c) symmetry fractionalisation of v. Recall that on the bonds $[U, \Lambda] = [V, \Lambda] = 0$.

Using the geometric series $\sum_{r=0}^{m-1} \omega^{rm'} = \frac{1-\omega^{mm'}}{1-\omega^{m'}}$ yields

$$\widehat{S}_j^{(m)} \left| v_j^{(a)} \right\rangle = \left(1 - \sum_{r=0}^{m-1} \frac{2}{N} \sum_{m'=0}^{N-1} \omega^{rm'} X_n^{m'} \right) \left| v_j^{(a)} \right\rangle = \left(1 - 2 \sum_{r=0}^{m-1} \delta_{r-a,0} \right) \left| v_j^{(a)} \right\rangle . \qquad (A.21)$$

Comparing with (A.20) and noting that $m < N$ yields (A.18). One can also derive the right-hand-side of (A.18) from the left-hand-side by taking products of (A.20) for different values of r and using (A.16).

Analogous identities hold with the replacement $X_n \to Z_n^{-1} Z_{n+1}$; the latter gives a sign, but one that depends on the difference of the states on the two sites as in (A.8). In particular,

$$\prod_{r=0}^{m-1} \Phi_{j-1,j}^{(r)} = S_{j-1,j}^{(m)} \equiv \left(1 - \frac{2m}{N} - \frac{2}{N} \sum_{m'=1}^{N-1} \alpha_{m'} \left(1 - \omega^{mm'}\right) Z_{j-1}^{-m'} Z_j^{m'} \right), \qquad (A.22)$$

leading to (17).

B String order and parity transformations

In this appendix we will show, following Ref. [69], that the charge of endpoints of string operators with long-range order reveals the SPT order for a $\mathbb{Z}_2 \times \mathbb{Z}_2^{\mathrm{CPT}}$ symmetry. The usual arguments are modified due to the $\mathbb{Z}_2^{\mathrm{CPT}}$ acting non-trivially on the lattice (through the parity transformation). In Figs. 8 and 9 we review the usual argument for the $\mathbb{Z}_2 \times \mathbb{Z}_2$ case graphically. Our analysis follows similar steps, but we use tensor notation to make the index transposition explicit. In this appendix we allow a more general representation of $\mathbb{Z}_2 \times \mathbb{Z}_2^{\mathrm{CPT}}$ than needed for the models in the main text. For technical reasons, we also assume translation invariance.

First, let us define a *symmetry flux* for the $\mathbb{Z}_2$ symmetry $\prod_j u_j$ by

$$\Sigma_n = \prod_{j \leq n} u_j \mathcal{O}_{n+1,\ldots,n+k}, \qquad (B.1)$$

where we require that the end-point $\mathcal{O}$ is Hermitian, and note that $u_n^2 = 1 \implies u_n^\dagger = u_n$. The end-point is required to be Hermitian so that there is no remaining phase freedom that would leave the charge under the anti-unitary CPT symmetry ill-defined [6]. The symmetry flux for a particular ground state is the half-infinite symmetry string with end-point such that the two-point function has the slowest possible decay—for gapped phases of matter this is the case with long-range order.

For an end-point operator $\mathcal{O}$ supported on k sites, we require that $\mathcal{O}u^{\otimes k} = u^{\otimes k}\mathcal{O}$ (this is the case in the main text, with $k = 2$). Note that this commutativity is equivalent to Σ_n being neutral under the $\mathbb{Z}_2$ symmetry. Moreover, this is equivalent to $\mathcal{O}u^{\otimes k}$ being Hermitian, implying that the string-order $\Sigma_1 \Sigma_n$ is Hermitian.
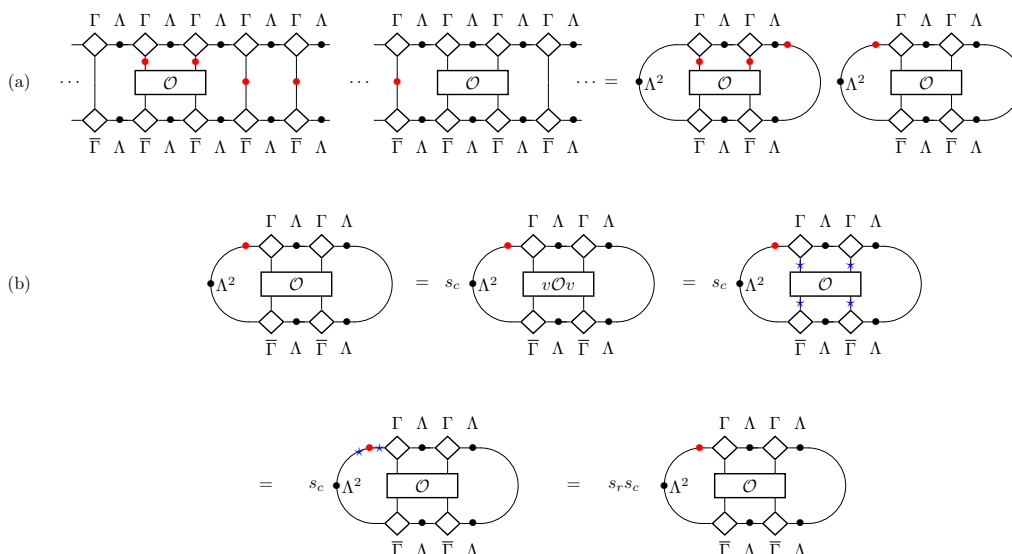
Figure 9: Graphical proof, following [69], that long-range string order with a charged end-point is non-vanishing only in the SPT phase for $\mathbb{Z}_2 \times \mathbb{Z}_2$ symmetry. In the text we generalise this to the $\mathbb{Z}_2 \times \mathbb{Z}_2^{\text{CPT}}$ case. The $\bullet$ indicate the symmetry u, and the $\star$ indicate the symmetry v (in the appropriate representation for either physical or bond indices). (a) The string order written as a tensor contraction using the MPS ground state, we apply Fig. 8(a) to simplify this to two local tensor contractions (the equality holds up to exponentially small corrections in the string length). Using Fig. 8(b) these terms are identical. (b) Analysing the local tensor contraction using the charge of the end-point $v\mathcal{O}v = s_c\mathcal{O}$ and the SPT phase $VUV = s_rU$. If the signs do not match then the string-order must vanish.

We are interested in end-point operators with a charge under the other symmetry $\mathbb{Z}_2^{\text{CPT}}$, where the charge is relative to multiplication by $u^{\otimes k}$. That is,

$$\mathcal{CPK} \, \mathcal{O} \, \mathcal{CPK} = s_{\text{c}} u^{\otimes k}\mathcal{O} \equiv s_{\text{c}}\tilde{\mathcal{O}}, \qquad s_{\text{c}} = \pm 1, \tag{B.2}$$

where we define $\tilde{\mathcal{O}} = u^{\otimes k}\mathcal{O}$ for convenience. As in the main text, we note that the parity symmetry $\mathcal{P}$ will translate the support of the operator in general. We suppose $\mathcal{C} = \prod_j C_j$ is a product of an on-site unitary involution that is real in the Z-basis.[5] This operation corresponds to applying the symmetry and then multiplying the inverted (B.1) by the $\mathbb{Z}_2$ symmetry $\prod_j u_j$ so that we can compare the end-point of the same half-infinite string. This multiplication by $u^{\otimes k}$ also arises naturally in the MPS formalism, as we demonstrate in the proof below.

The string order is the two-point correlator of the (Hermitian) symmetry flux (B.1)

$$\langle \Sigma_1 \Sigma_M \rangle = \langle \tilde{\mathcal{O}}_{1,2,\dots,k} \left(\prod_{j=k+1}^{M} u_j \right) \mathcal{O}_{M+1,\dots,M+k} \rangle. \tag{B.3}$$

Let s_{c} be the charge of the end-point and let s_{r} be the invariant charge of the projective representation of $\mathbb{Z}_2 \times \mathbb{Z}_2^{\text{CPT}}$ on the virtual degrees of freedom ($UV = s_{\text{r}}VU$). Assuming a symmetric

---

[5]Without loss of generality we can take our inversion $\mathcal{P}$ to be real. We expect a similar argument to go through if we consider the more general case $\mathcal{CPK} \, \mathcal{O} \, \overline{\mathcal{CPK}} = \pm\tilde{\mathcal{O}}$, since the $\mathbb{Z}_2$ implies $(\mathcal{CP})^\dagger = \overline{\mathcal{CP}}$. Moreover, an analogous charge and selection rule applies in the case where we have a $\mathbb{Z}_2^P$ or $\mathbb{Z}_2^{CP}$ symmetry that includes a parity transformation but does not include time-reversal.

ground state, we have the selection rule:

$$\lim_{M,L\to\infty} \langle \Sigma_1 \Sigma_M \rangle = x^2, \qquad \text{for } x \in \mathbb{R},$$

$$\text{and} \qquad x = s_c s_r x. \tag{B.4}$$

This means that the long-range string order is non-vanishing only if $s_c = s_r$, giving us a method of detecting the SPT phase with a lattice observable.

B.1 Proof of string order selection rule

We derive (B.4) using the MPS formalism; using the area law for ground states of gapped local Hamiltonians in 1D to justify using these results more generally [13,108]. The outline of the proof is roughly given in Fig. 9; the complication is the inclusion of the time-reversal and parity transformations. Together, these act on the MPS tensors to take $\Gamma \to \Gamma^\dagger$, allowing us to use the symmetry fractionalisation of $\mathcal{C}$ as in Fig. 9(b). Our argument uses translation-invariance, and we will use this translation symmetry when we act with the $\mathcal{P}$ symmetry on the local tensor contraction (denoted x below)—in particular, we will choose $\mathcal{P}$ to invert about the central bond (or site) of the support of $\tilde{\mathcal{O}}$.

Take a (translation-invariant) MPS representation of the ground state, with tensors $\mathcal{A}_j$ in canonical form. We can write the correlator in terms of the generalised transfer matrix $E_\mathcal{X} = \sum_{j,j'=0}^{N-1} \mathcal{X}_{j'j} \mathcal{A}_j \otimes \mathcal{A}_{j'}^\dagger$ (with the natural generalisation to operators supported on multiple sites). We then have

$$\langle \Sigma_1 \Sigma_M \rangle = \text{tr} \left(E_{\mathbb{I}}^{L-M-k} E_{\tilde{\mathcal{O}}} E_u^{M-k} E_{\mathcal{O}} \right), \tag{B.5}$$

which can be simplified (up to exponentially small corrections) for large chain length, L, and large string length, M, as

$$\langle \Sigma_1 \Sigma_M \rangle \simeq \underbrace{\langle \Lambda^2 | E_{\tilde{\mathcal{O}}} | U \rangle}_{x} \underbrace{\langle \Lambda^2 U | E_{\mathcal{O}} | \mathbb{I} \rangle}_{y}. \tag{B.6}$$

This follows from the implicit assumption that the unique dominant eigenvalue of $E_{\mathbb{I}}$ is equal to one, and that $\sum_{j'} u_{jj'} \mathcal{A}_{j'}$ fractionalises to $U\mathcal{A}_j U$ on the bonds (we can fix the phase so that $U = U^\dagger$ since we have a representation of $\mathbb{Z}_2$). This can be seen graphically for $k = 2$ in Fig. 9(a).

The non-vanishing of the string order means that neither of the two factors in (B.6) vanishes. We will show first that these factors are both equal to the same real number. That is, $x = y \in \mathbb{R}$ (the equality is straightforward to see graphically, as in Fig. 9(a)). We then show that a charged endpoint will cause x to vanish unless there is a non-trivial projective representation of $\mathbb{Z}_2 \times \mathbb{Z}_2^{\text{CPT}}$ on the bonds. This is in line with the string order for an on-site $\mathbb{Z}_2 \times \mathbb{Z}_2$ symmetry [69].

Define the matrix $\tilde{M}^{\gamma\delta} = \left[\langle \Lambda^2 | E_{\tilde{\mathcal{O}}} \right]^{\gamma\delta}$, then

$$\tilde{M}^{\gamma\delta} = \sum \Lambda_\alpha^2 \mathcal{A}_{j_1}^{\alpha\beta_1} \overline{\mathcal{A}}_{j_1'}^{\alpha\beta_1'} \left(\prod_{m=1}^{k-2} \mathcal{A}_{j_{m+1}}^{\beta_m\beta_{m+1}} \overline{\mathcal{A}}_{j_{m+1}'}^{\beta_m'\beta_{m+1}'} \right) \mathcal{A}_{j_k}^{\beta_k\gamma} \overline{\mathcal{A}}_{j_k'}^{\beta_k\delta} \tilde{\mathcal{O}}_{j_1\cdots j_k, j_1'\cdots j_k'} \tag{B.7}$$

(where we sum over all indices except γ and δ). Then $x = \langle \Lambda^2 | E_{\tilde{\mathcal{O}}} | U \rangle = \text{tr}(\tilde{M}U)$. Now, we have that $\overline{x} = \overline{\langle \Lambda^2 | E_{\tilde{\mathcal{O}}} | U \rangle} = \text{tr}(\tilde{M}^\dagger U)$. Using that $\tilde{\mathcal{O}} = \tilde{\mathcal{O}}^\dagger$ we have that $\tilde{M}^\dagger = \tilde{M}$ and so $x \in \mathbb{R}$. We also have from symmetry fractionalisation that $\sum_\beta \mathcal{A}_j^{\alpha\beta} U^{\beta\gamma} = \sum_{\beta,\tilde{j}} u_{j,\tilde{j}} U^{\alpha\beta} \mathcal{A}_{\tilde{j}}^{\beta\gamma}$. We can then move the U to the left, at each step applying u to the physical index. This gives us that $x = \text{tr}(\tilde{M}U) = \text{tr}(M)$ where $M^{\gamma\delta} = \left[\langle \Lambda^2 U | E_{\mathcal{O}} \right]^{\gamma\delta}$; i.e.

$$M^{\gamma\delta} = \sum \Lambda_\alpha^2 U^{\alpha\alpha'} \mathcal{A}_{j_1}^{\alpha'\beta_1} \overline{\mathcal{A}}_{j_1'}^{\alpha\beta_1'} \left(\prod_{m=1}^{k-2} \mathcal{A}_{j_{m+1}}^{\beta_m\beta_{m+1}} \overline{\mathcal{A}}_{j_{m+1}'}^{\beta_m'\beta_{m+1}'} \right) \mathcal{A}_{j_k}^{\beta_k\gamma} \overline{\mathcal{A}}_{j_k'}^{\beta_k\delta} \mathcal{O}_{j_1\cdots j_k, j_1'\cdots j_k'}. \tag{B.8}$$

We recognise the trace of M as y, and hence both factors in (B.6) are equal to $x \in \mathbb{R}$.

The symmetry fractionalisation of $\mathbb{Z}_2^{\mathrm{CPT}}$ is

$$\sum_{j'=0}^{N-1} C_{j,j'} (\Gamma_{j'}^{\alpha,\beta})^\dagger = V \, \Gamma_j^{\alpha,\beta} \, V \,, \tag{B.9}$$

where we decompose $\mathcal{A}_j^{\alpha,\beta} = \Gamma_j^{\alpha,\beta} \Lambda_\beta$. Again, since $C^2 = \mathbb{I}$ we can fix the phase so that $V = V^\dagger$. Just as in the on-site $\mathbb{Z}_2 \times \mathbb{Z}_2$ case, $UV = s_\mathrm{r} VU$ is a gauge invariant phase that determines the SPT order.

Now, using $x = \overline{x} = \mathrm{tr}(M)$ and $U = U^\dagger$ we have

$$x = \sum \Lambda_\alpha^2 U^{\alpha'\alpha} \overline{\mathcal{A}}_{j_1}^{\alpha'\beta_1} \mathcal{A}_{j_1'}^{\alpha\beta_1'} \left(\prod_{m=1}^{k-2} \overline{\mathcal{A}}_{j_{m+1}}^{\beta_m\beta_{m+1}} \mathcal{A}_{j_{m+1}'}^{\beta_m'\beta_{m+1}'} \right) \overline{\mathcal{A}}_{j_k}^{\beta_k\gamma} \mathcal{A}_{j_k'}^{\beta_k\gamma} \overline{\mathcal{O}}_{j_1\cdots j_k, j_1'\cdots j_k'} . \tag{B.10}$$

Inserting $\mathbb{I} = \mathcal{P}^2$ on the physical indices we have:

$$x = \sum \mathcal{A}_{j_1}^{\dagger\alpha\beta_1} \mathcal{A}_{j_1'}^{T\,\alpha\beta_1'} \left(\prod_{m=1}^{k-2} \mathcal{A}_{j_{m+1}}^{\dagger\beta_m\beta_{m+1}} \mathcal{A}_{j_{m+1}'}^{T\beta_m'\beta_{m+1}'} \right) \mathcal{A}_{j_k}^{\dagger\beta_k\gamma} \mathcal{A}_{j_k'}^{T\beta_k\gamma'} U^{\gamma\gamma'} \Lambda_\gamma^2 \, (\mathcal{P}\overline{\mathcal{O}}\mathcal{P})_{j_1\cdots j_k, j_1'\cdots j_k'} . \tag{B.11}$$

Finally inserting $\mathbb{I} = \mathcal{C}^2$ gives

$$x = \sum \Lambda_\alpha^2 \mathcal{A}_{j_1}^{\alpha\beta_1} \overline{\mathcal{A}}_{j_1'}^{\alpha\beta_1'} \left(\prod_{m=1}^{k-2} \mathcal{A}_{j_{m+1}}^{\beta_m\beta_{m+1}} \overline{\mathcal{A}}_{j_{m+1}'}^{\beta_m'\beta_{m+1}'} \right) \mathcal{A}_{j_k}^{\beta_k\gamma} \overline{\mathcal{A}}_{j_k'}^{\beta_k\gamma'} (VUV)^{\gamma\gamma'} \, (\mathcal{C}\mathcal{P}\overline{\mathcal{O}}\mathcal{P}\mathcal{C})_{j_1\cdots j_k, j_1'\cdots j_k'} . \tag{B.12}$$

Comparing this expression to $x = \mathrm{tr}(\tilde{M}U)$ we see that $x = s_\mathrm{c} s_\mathrm{r} x$ as claimed.

B.2 String order for $N = 4$

In Section 5.3 we write the string order (50) in terms of the simple string correlators:

$$S_{a,b} = \lim_{M,L\to\infty} \langle Z_1^a Z_2^{-a} X_2^2 \cdots X_M^2 Z_M^b Z_{M+1}^{-b} \rangle . \tag{B.13}$$

Multiplying out the terms that appear for $N = 4$, the string order (50) is equal to

$$\lim_{M,L\to\infty} \langle \tilde{\mathcal{O}}_{0,1} \left(\prod_{j=2}^{M-1} X_j^{N/2} \right) \mathcal{O}_{M,M+1} \rangle = \frac{i}{2} \left(S_{-1,-1} - S_{1,1} \right) + \frac{1}{2} \left(S_{-1,1} + S_{1,-1} \right) . \tag{B.14}$$

Using the same MPS transfer matrix arguments as in the previous subsection we have that $S_{a,b}$ is equal to $M^{(a)} \tilde{M}^{(b)}$, where

$$M^{(a)} = \sum \Lambda_\alpha^2 \mathcal{A}_{j_1}^{\alpha\beta_1} \overline{\mathcal{A}}_{j_1'}^{\alpha\beta_1'} \mathcal{A}_{j_2}^{\beta_1\gamma} \overline{\mathcal{A}}_{j_2'}^{\beta_1'\delta} Z_{j_1,j_1'}^a (Z^{-a} X^2)_{j_2,j_2'} U^{\gamma\delta} \,, \tag{B.15}$$

$$\tilde{M}^{(b)} = \sum \Lambda_\alpha^2 U^{\alpha\alpha'} \mathcal{A}_{j_1}^{\alpha\beta_1} \overline{\mathcal{A}}_{j_1'}^{\alpha'\beta_1'} \mathcal{A}_{j_2}^{\beta_1\gamma} \overline{\mathcal{A}}_{j_2'}^{\beta_1'\delta} (X^2 Z^b)_{j_1,j_1'} Z_{j_2,j_2'}^{-b} \,. \tag{B.16}$$

U is the fractionalised $\mathbb{Z}_2$ symmetry that acts as X^2 on physical indices. Using symmetry fractionalisation and that $X^2 Z^{\pm 1} = -Z^{\pm 1} X^2$ we have that $M^{(a)} = -\tilde{M}^{(a)}$.

Conjugating $M^{(a)}$ amounts to taking the Hermitian conjugate of the physical operator. Since we have $(Z_1^a Z_2^{-a} X_2^2)^\dagger = -Z_1^{-a} Z_2^a X_2^2$, we conclude that $\overline{M}^{(a)} = -M^{(-a)}$. Putting this together

$$\lim_{R\to\infty} \langle \tilde{\mathcal{O}}_{0,1} \left(\prod_{j=2}^{R-1} X_j^{N/2} \right) \mathcal{O}_{R,R+1} \rangle = -\mathrm{Im}(M^{(-1)}\overline{M}^{(1)}) + \frac{1}{2} \left(|M^{(-1)}|^2 + |M^{(1)}|^2 \right)$$

$$= \frac{i}{2} \left(S_{-1,-1} - S_{1,1} \right) + S_{-1,1} \,. \tag{B.17}$$

Using the fixed-point MPS (37), one can show explicitly that $\text{Re}(M^{(1)}) = -\text{Im}(M^{(1)})$. At the fixed-point this means that the string correlator

$$1 = \lim_{R \to \infty} \langle \tilde{\mathcal{O}}_{0,1} \bigg(\prod_{j=2}^{R-1} X_j^{N/2} \bigg) \mathcal{O}_{R,R+1} \rangle = 2S_{-1,1} \,.$$

According to our numerics, this relationship continues to hold away from the fixed point. It would be interesting to establish this analytically using the projective representations.

References

[1] X.-G. Wen, *Colloquium: Zoo of quantum-topological phases of matter*, Rev. Mod. Phys. **89**, 041004 (2017), doi:10.1103/RevModPhys.89.041004.

[2] F. Duncan and M. Haldane, *Nobel lecture: Topological quantum matter*, Rev. Mod. Phys. **89**, 040502 (2017), doi:10.1103/RevModPhys.89.040502.

[3] H. A. Kramers and G. H. Wannier, *Statistics of the two-dimensional ferromagnet. Part I*, Phys. Rev. **60**, 252 (1941), doi:10.1103/PhysRev.60.252.

[4] X. Chen, Y.-M. Lu and A. Vishwanath, *Symmetry-protected topological phases from decorated domain walls*, Nat. Commun. **5**, 3507 (2014), doi:10.1038/ncomms4507.

[5] R. Verresen, R. Moessner and F. Pollmann, *One-dimensional symmetry protected topological phases and their transitions*, Phys. Rev. B **96**, 165124 (2017), doi:10.1103/PhysRevB.96.165124.

[6] R. Verresen, R. Thorngren, N. G. Jones and F. Pollmann, *Gapless topological phases and symmetry-enriched quantum criticality*, Phys. Rev. X **11**, 041059 (2021), doi:10.1103/PhysRevX.11.041059.

[7] N. Tantivasadakarn, R. Thorngren, A. Vishwanath and R. Verresen, *Pivot Hamiltonians as generators of symmetry and entanglement*, SciPost Phys. **14**, 012 (2023), doi:10.21468/SciPostPhys.14.2.012.

[8] C. Zhang, *Topological invariants for symmetry-protected topological phase entanglers*, Phys. Rev. B **107**, 235104 (2023), doi:10.1103/PhysRevB.107.235104.

[9] N. Tantivasadakarn, R. Thorngren, A. Vishwanath and R. Verresen, *Building models of topological quantum criticality from pivot Hamiltonians*, SciPost Phys. **14**, 013 (2023), doi:10.21468/SciPostPhys.14.2.013.

[10] N. Schuch, D. Pérez-García and I. Cirac, *Classifying quantum phases using matrix product states and projected entangled pair states*, Phys. Rev. B **84**, 165139 (2011), doi:10.1103/PhysRevB.84.165139.

[11] C.-K. Chiu, J. C. Y. Teo, A. P. Schnyder and S. Ryu, *Classification of topological quantum matter with symmetries*, Rev. Mod. Phys. **88**, 035005 (2016), doi:10.1103/RevModPhys.88.035005.

[12] B. Zeng, X. Chen, D.-L. Zhou and X.-G. Wen, *Quantum information meets quantum matter*, Springer, New York, USA, ISBN 9781493990825 (2019), doi:10.1007/978-1-4939-9084-9.

[13] J. I. Cirac, D. Pérez-García, N. Schuch and F. Verstraete, *Matrix product states and projected entangled pair states: Concepts, symmetries, theorems*, Rev. Mod. Phys. **93**, 045003 (2021), doi:10.1103/RevModPhys.93.045003.

[14] R. Raussendorf, D. E. Browne and H. J. Briegel, *Measurement-based quantum computation on cluster states*, Phys. Rev. A **68**, 022312 (2003), doi:10.1103/PhysRevA.68.022312.

[15] W. Son, L. Amico, R. Fazio, A. Hamma, S. Pascazio and V. Vedral, *Quantum phase transition between cluster and antiferromagnetic states*, Europhys. Lett. **95**, 50001 (2011), doi:10.1209/0295-5075/95/50001.

[16] L. Onsager, *Crystal statistics. I. A two-dimensional model with an order-disorder transition*, Phys. Rev. **65**, 117 (1944), doi:10.1103/PhysRev.65.117.

[17] B. Davies, *Onsager's algebra and superintegrability*, J. Phys. A: Math. Gen. **23**, 2245 (1990), doi:10.1088/0305-4470/23/12/010.

[18] B. Davies, *Onsager's algebra and the Dolan-Grady condition in the non-self-dual case*, J. Math. Phys. **32**, 2945 (1991), doi:10.1063/1.529036.

[19] L. Dolan and M. Grady, *Conserved charges from self-duality*, Phys. Rev. D **25**, 1587 (1982), doi:10.1103/PhysRevD.25.1587.

[20] G. von Gehlen and V. Rittenberg, Z_n-*symmetric quantum chains with an infinite set of conserved charges and* Z_n *zero modes*, Nucl. Phys. B **257**, 351 (1985), doi:10.1016/0550-3213(85)90350-5.

[21] C. Ahn and K. Shigemoto, *Onsager algebra and integrable lattice models*, Mod. Phys. Lett. A **06**, 3509 (1991), doi:10.1142/S021773239100405X.

[22] H. Au-Yang, B. M. McCoy, J. H. H. Perk, S. Tang and M.-L. Yan, *Commuting transfer matrices in the chiral Potts models: Solutions of star-triangle equations with genus>1*, Phys. Lett. A **123**, 219 (1987), doi:10.1016/0375-9601(87)90065-X.

[23] E. O'Brien, E. Vernier and P. Fendley, *"Not-A", representation symmetry-protected topological, and Potts phases in an* S_3-*invariant chain*, Phys. Rev. B **101**, 235108 (2020), doi:10.1103/PhysRevB.101.235108.

[24] F. Pollmann, E. Berg, A. M. Turner and M. Oshikawa, *Symmetry protection of topological phases in one-dimensional quantum spin systems*, Phys. Rev. B **85**, 075125 (2012), doi:10.1103/PhysRevB.85.075125.

[25] R. Verresen, P. Fendley and N. Tantivasadakarn, *In preparation*.

[26] F. Anfuso and A. Rosch, *String order and adiabatic continuity of Haldane chains and band insulators*, Phys. Rev. B **75**, 144420 (2007), doi:10.1103/PhysRevB.75.144420.

[27] S. Moudgalya and F. Pollmann, *Fragility of symmetry-protected topological order on a Hubbard ladder*, Phys. Rev. B **91**, 155128 (2015), doi:10.1103/PhysRevB.91.155128.

[28] Z. Bi and T. Senthil, *Adventure in topological phase transitions in* $3 + 1$-*D: Non-Abelian deconfined quantum criticalities and a possible duality*, Phys. Rev. X **9**, 021034 (2019), doi:10.1103/PhysRevX.9.021034.

[29] C.-M. Jian and C. Xu, *Generic "unnecessary" quantum critical points with minimal degrees of freedom*, Phys. Rev. B **101**, 035118 (2020), doi:10.1103/PhysRevB.101.035118.

[30] R. Verresen, J. Bibo and F. Pollmann, *Quotient symmetry protected topological phenomena*, (arXiv preprint) doi:10.48550/arXiv.2102.08967.

[31] A. Prakash, M. Fava and S. A. Parameswaran, *Multiversality and unnecessary criticality in one dimension*, Phys. Rev. Lett. **130**, 256401 (2023), doi:10.1103/PhysRevLett.130.256401.

[32] A. Prakash and N. G. Jones, *Classical origins of Landau-incompatible transitions*, Phys. Rev. Lett. **134**, 097103 (2025), doi:10.1103/PhysRevLett.134.097103.

[33] S. Howes, L. P. Kadanoff and M. Den Nijs, *Quantum model for commensurate-incommensurate transitions*, Nucl. Phys. B **215**, 169 (1983), doi:10.1016/0550-3213(83)90212-2.

[34] G. Albertini, B. M. McCoy and J. H. H. Perk, *Level crossing transitions and the massless phases of the superintegrable chiral Potts chain*, Phys. Lett. A **139**, 204 (1989), doi:10.1016/0375-9601(89)90142-4.

[35] G. Albertini, B. M. McCoy and J. H. Perk, *Eigenvalue spectrum of the superintegrable chiral Potts model*, in *Integrable systems in quantum field theory and statistical mechanics*, Academic Press, San Diego, USA, ISBN 9780123853424 (1989), doi:10.1016/B978-0-12-385342-4.50007-X.

[36] S. Mondal, A. Agarwala, T. Mishra and A. Prakash, *Symmetry-enriched criticality in a coupled spin ladder*, Phys. Rev. B **108**, 245135 (2023), doi:10.1103/PhysRevB.108.245135.

[37] P. Fendley, N. G. Jones and A. Prakash, *In preparation*.

[38] E. Vernier, E. O'Brien and P. Fendley, *Onsager symmetries in $U(1)$-invariant clock models*, J. Stat. Mech.: Theory Exp. 043107 (2019), doi:10.1088/1742-5468/ab11c0.

[39] R. Raussendorf and T.-C. Wei, *Quantum computation by local measurement*, Annu. Rev. Condens. Matter Phys. **3**, 239 (2012), doi:10.1146/annurev-conmatphys-020911-125041.

[40] A. Prakash and T.-C. Wei, *Ground states of one-dimensional symmetry-protected topological phases and their utility as resource states for quantum computation*, Phys. Rev. A **92**, 022310 (2015), doi:10.1103/physreva.92.022310.

[41] D. T. Stephen, D.-S. Wang, A. Prakash, T.-C. Wei and R. Raussendorf, *Computational power of symmetry-protected topological phases*, Phys. Rev. Lett. **119**, 010504 (2017), doi:10.1103/physrevlett.119.010504.

[42] R. Raussendorf, D.-S. Wang, A. Prakash, T.-C. Wei and D. T. Stephen, *Symmetry-protected topological phases with uniform computational power in one dimension*, Phys. Rev. A **96**, 012302 (2017), doi:10.1103/physreva.96.012302.

[43] Y. Chen, A. Prakash and T.-C. Wei, *Universal quantum computing using $(\mathbb{Z}_d)^3$ symmetry-protected topologically ordered states*, Phys. Rev. A **97**, 022305 (2018), doi:10.1103/PhysRevA.97.022305.

[44] M. Suzuki, *Relationship among exactly soluble models of critical phenomena. I*, Prog. Theor. Phys. **46**, 1337 (1971), doi:10.1143/PTP.46.1337.

[45] J. P. Keating and F. Mezzadri, *Random matrix theory and entanglement in quantum spin chains*, Commun. Math. Phys. **252**, 543 (2004), doi:10.1007/s00220-004-1188-2.

[46] P. Smacchia, L. Amico, P. Facchi, R. Fazio, G. Florio, S. Pascazio and V. Vedral, *Statistical mechanics of the cluster Ising model*, Phys. Rev. A **84**, 022304 (2011), doi:10.1103/PhysRevA.84.022304.

[47] W. DeGottardi, M. Thakurathi, S. Vishveshwara and D. Sen, *Majorana fermions in super-conducting wires: Effects of long-range hopping, broken time-reversal symmetry, and potential landscapes*, Phys. Rev. B **88**, 165111 (2013), doi:10.1103/PhysRevB.88.165111.

[48] T. Ohta, S. Tanaka, I. Danshita and K. Totsuka, *Topological and dynamical properties of a generalized cluster model in one dimension*, Phys. Rev. B **93**, 165423 (2016), doi:10.1103/PhysRevB.93.165423.

[49] R. Verresen, N. G. Jones and F. Pollmann, *Topology and edge modes in quantum critical chains*, Phys. Rev. Lett. **120**, 057001 (2018), doi:10.1103/PhysRevLett.120.057001.

[50] T. Prosen, *Exact time-correlation functions of quantum Ising chain in a kicking transversal magnetic field*, Prog. Theor. Phys. Suppl. **139**, 191 (2000), doi:10.1143/PTPS.139.191.

[51] W. Magnus, *On the exponential solution of differential equations for a linear operator*, Commun. Pure Appl. Math. **7**, 649 (1954), doi:10.1002/cpa.3160070404.

[52] D. Aasen, P. Fendley and R. S. K. Mong, *Topological defects on the lattice: Dualities and degeneracies*, (arXiv preprint) doi:10.48550/arXiv.2008.08598.

[53] R. J. Baxter, *Free energy of the solvable chiral Potts model*, J. Stat. Phys. **52**, 639 (1988), doi:10.1007/BF01019722.

[54] R. J. Baxter, *Superintegrable chiral Potts model: Thermodynamic properties, an "inverse model", and a simple associated Hamiltonian*, J. Stat. Phys. **57**, 1 (1989), doi:10.1007/BF01023632.

[55] E. Cobanera, G. Ortiz and Z. Nussinov, *The bond-algebraic approach to dualities*, Adv. Phys. **60**, 679 (2011), doi:10.1080/00018732.2011.619814.

[56] N. Moran, D. Pellegrino, J. K. Slingerland and G. Kells, *Parafermionic clock models and quantum resonance*, Phys. Rev. B **95**, 235127 (2017), doi:10.1103/PhysRevB.95.235127.

[57] S. Whitsitt, R. Samajdar and S. Sachdev, *Quantum field theory for the chiral clock transition in one spatial dimension*, Phys. Rev. B **98**, 205118 (2018), doi:10.1103/PhysRevB.98.205118.

[58] Y. Yoo and B. Swingle, *Temperature dependence of energy transport in the $\mathbb{Z}_3$ chiral clock model*, Phys. Rev. B **109**, 235104 (2024), doi:10.1103/PhysRevB.109.235104.

[59] X. Chen, Z.-C. Gu and X.-G. Wen, *Classification of gapped symmetric phases in one-dimensional spin systems*, Phys. Rev. B **83**, 035107 (2011), doi:10.1103/PhysRevB.83.035107.

[60] T. Scaffidi, D. E. Parker and R. Vasseur, *Gapless symmetry-protected topological order*, Phys. Rev. X **7**, 041048 (2017), doi:10.1103/PhysRevX.7.041048.

[61] S. D. Geraedts and O. I. Motrunich, *Exact models for symmetry-protected topological phases in one dimension*, (arXiv preprint) doi:10.48550/arXiv.1410.1580.

[62] A. Prakash, C. G. West and T.-C. Wei, *Detection of gapped phases of a one-dimensional spin chain with on-site and spatial symmetries*, Phys. Rev. B **94**, 045136 (2016), doi:10.1103/PhysRevB.94.045136.

[63] C. Zhang and M. Levin, *Exactly solvable model for a deconfined quantum critical point in 1D*, Phys. Rev. Lett. **130**, 026801 (2023), doi:10.1103/PhysRevLett.130.026801.

[64] L. Su, *Boundary criticality via gauging finite subgroups: A case study on the clock model*, (arXiv preprint) doi:10.48550/arXiv.2306.02976.

[65] L. Su and M. Zeng, *Gapless symmetry-protected topological phases and generalized deconfined critical points from gauging a finite subgroup*, Phys. Rev. B **109**, 245108 (2024), doi:10.1103/PhysRevB.109.245108.

[66] X. Chen, Z.-C. Gu, Z.-X. Liu and X.-G. Wen, *Symmetry protected topological orders and the group cohomology of their symmetry group*, Phys. Rev. B **87**, 155114 (2013), doi:10.1103/PhysRevB.87.155114.

[67] G. De las Cuevas, J. I. Cirac, N. Schuch and D. Perez-Garcia, *Irreducible forms of matrix product states: Theory and applications*, J. Math. Phys. **58**, 121901 (2017), doi:10.1063/1.5000784.

[68] D. Pérez-García, M. M. Wolf, M. Sanz, F. Verstraete and J. I. Cirac, *String order and symmetries in quantum spin lattices*, Phys. Rev. Lett. **100**, 167202 (2008), doi:10.1103/PhysRevLett.100.167202.

[69] F. Pollmann and A. M. Turner, *Detection of symmetry-protected topological phases in one dimension*, Phys. Rev. B **86**, 125441 (2012), doi:10.1103/PhysRevB.86.125441.

[70] G. Vidal, *Classical simulation of infinite-size quantum lattice systems in one spatial dimension*, Phys. Rev. Lett. **98**, 070201 (2007), doi:10.1103/PhysRevLett.98.070201.

[71] F. Pollmann, A. M. Turner, E. Berg and M. Oshikawa, *Entanglement spectrum of a topological phase in one dimension*, Phys. Rev. B **81**, 064439 (2010), doi:10.1103/PhysRevB.81.064439.

[72] A. M. Turner, Y. Zhang and A. Vishwanath, *Entanglement and inversion symmetry in topological insulators*, Phys. Rev. B **82**, 241102 (2010), doi:10.1103/PhysRevB.82.241102.

[73] F. Pollmann, E. Berg, A. M. Turner and M. Oshikawa, *Symmetry protection of topological phases in one-dimensional quantum spin systems*, Phys. Rev. B **85**, 075125 (2012), doi:10.1103/PhysRevB.85.075125.

[74] E. Khalaf, W. A. Benalcazar, T. L. Hughes and R. Queiroz, *Boundary-obstructed topological phases*, Phys. Rev. Res. **3**, 013239 (2021), doi:10.1103/PhysRevResearch.3.013239.

[75] L. P. Kadanoff and H. Ceva, *Determination of an operator algebra for the two-dimensional Ising model*, Phys. Rev. B **3**, 3918 (1971), doi:10.1103/PhysRevB.3.3918.

[76] S. Mondal, A. Agarwala, T. Mishra and A. Prakash, *Symmetry-enriched criticality in a coupled spin ladder*, Phys. Rev. B **108**, 245135 (2023), doi:10.1103/PhysRevB.108.245135.

[77] M. Fishman, S. White and E. Stoudenmire, *The ITensor software library for tensor network calculations*, SciPost Phys. Codebases 4 (2022), doi:10.21468/SciPostPhysCodeb.4.

[78] M. Fishman, S. White and E. Stoudenmire, *Codebase release 0.3 for ITensor*, SciPost Phys. Codebases 4-r0.3 (2022), doi:10.21468/SciPostPhysCodeb.4-r0.3.

[79] G. Albertini, B. M. McCoy and J. H. H. Perk, *Commensurate-incommensurate transition in the ground state of the superintegrable chiral Potts model*, Phys. Lett. A **135**, 159 (1989), doi:10.1016/0375-9601(89)90254-5.

[80] G. Albertini, B. M. McCoy, J. H. H. Perk and S. Tang, *Excitation spectrum and order parameter for the integrable N-state chiral Potts model*, Nucl. Phys. B **314**, 741 (1989), doi:10.1016/0550-3213(89)90415-X.

[81] B. M. McCoy and S.-s. Roan, *Excitation spectrum and phase structure of the chiral Potts model*, Phys. Lett. A **150**, 347 (1990), doi:10.1016/0375-9601(90)90230-L.

[82] Y. Zhuang, H. J. Changlani, N. M. Tubman and T. L. Hughes, *Phase diagram of the Z_3 parafermionic chain with chiral interactions*, Phys. Rev. B **92**, 035154 (2015), doi:10.1103/PhysRevB.92.035154.

[83] M. Rodney, H. F. Song, S.-S. Lee, K. Le Hur and E. S. Sørensen, *Scaling of entanglement entropy across Lifshitz transitions*, Phys. Rev. B **87**, 115132 (2013), doi:10.1103/PhysRevB.87.115132.

[84] G. Albertini and B. M. McCoy, *Correlation functions of the chiral Potts chain from conformal field theory and finite-size corrections*, Nucl. Phys. B **350**, 745 (1991), doi:10.1016/0550-3213(91)90162-Q.

[85] J. L. Cardy, *Critical exponents of the chiral Potts model from conformal field theory*, Nucl. Phys. B **389**, 577 (1993), doi:10.1016/0550-3213(93)90353-Q.

[86] L. Gioia and C. Wang, *Nonzero momentum requires long-range entanglement*, Phys. Rev. X **12**, 031007 (2022), doi:10.1103/PhysRevX.12.031007.

[87] R. J. Baxter, *Derivation of the order parameter of the chiral Potts model*, Phys. Rev. Lett. **94**, 130602 (2005), doi:10.1103/PhysRevLett.94.130602.

[88] R. J. Baxter, *The order parameter of the chiral Potts model*, J. Stat. Phys. **120**, 1 (2005), doi:10.1007/s10955-005-5534-3.

[89] S. Sachdev, *Quantum phase transitions*, Cambridge University Press, Cambridge, UK, ISBN 9780521514682 (2011), doi:10.1017/CBO9780511973765.

[90] E. Barouch and B. M. McCoy, *Statistical mechanics of the XY model. II. Spin-correlation functions*, Phys. Rev. A **3**, 786 (1971), doi:10.1103/PhysRevA.3.786.

[91] M. M. Wolf, G. Ortiz, F. Verstraete and J. I. Cirac, *Quantum phase transitions in matrix product systems*, Phys. Rev. Lett. **97**, 110403 (2006), doi:10.1103/PhysRevLett.97.110403.

[92] A. Smith, B. Jobst, A. G. Green and F. Pollmann, *Crossing a topological phase transition with a quantum computer*, Phys. Rev. Res. **4**, L022020 (2022), doi:10.1103/PhysRevResearch.4.L022020.

[93] N. G. Jones, J. Bibo, B. Jobst, F. Pollmann, A. Smith and R. Verresen, *Skeleton of matrix-product-state-solvable models connecting topological phases of matter*, Phys. Rev. Res. **3**, 033265 (2021), doi:10.1103/PhysRevResearch.3.033265.

[94] N. G. Jones and R. Verresen, *Exact correlations in topological quantum chains*, Symmetry Integr. Geom.: Methods Appl. **19**, 098 (2023), doi:10.3842/SIGMA.2023.098.

[95] J. Kurmann, H. Thomas and G. Müller, *Antiferromagnetic long-range order in the anisotropic quantum spin chain*, Phys. A: Stat. Mech. Appl. **112**, 235 (1982), doi:10.1016/0378-4371(82)90217-5.

[96] J. H. Taylor and G. Müller, *Limitations of spin-wave theory in $T = 0$ spin dynamics*, Phys. Rev. B **28**, 1529 (1983), doi:10.1103/PhysRevB.28.1529.

[97] G. Müller and R. E. Shrock, *Implications of direct-product ground states in the one-dimensional quantum XYZ and XY spin chains*, Phys. Rev. B **32**, 5845 (1985), doi:10.1103/PhysRevB.32.5845.

[98] S. R. White, *Density matrix formulation for quantum renormalization groups*, Phys. Rev. Lett. **69**, 2863 (1992), doi:10.1103/PhysRevLett.69.2863.

[99] H. Li and F. D. M. Haldane, *Entanglement spectrum as a generalization of entanglement entropy: Identification of topological order in non-Abelian fractional quantum Hall effect states*, Phys. Rev. Lett. **101**, 010504 (2008), doi:10.1103/PhysRevLett.101.010504.

[100] P. Calabrese and J. Cardy, *Entanglement entropy and quantum field theory*, J. Stat. Mech.: Theory Exp. P06002 (2004), doi:10.1088/1742-5468/2004/06/P06002.

[101] P. Ginsparg, *Applied conformal field theory*, in *Fields, strings and critical phenomena: Proceedings*, Elsevier, Amsterdam, Netherlands, ISBN 9780444884404 (1989).

[102] J. Fjelstad and T. Månsson, *New symmetries of the chiral Potts model*, J. Phys. A: Math. Theor. **45**, 155208 (2012), doi:10.1088/1751-8113/45/15/155208.

[103] K. Minami, *Onsager algebra and algebraic generalization of Jordan-Wigner transformation*, Nucl. Phys. B **973**, 115599 (2021), doi:10.1016/j.nuclphysb.2021.115599.

[104] Y. Miao, *Conjectures on hidden Onsager algebra symmetries in interacting quantum lattice models*, SciPost Phys. **11**, 066 (2021), doi:10.21468/SciPostPhys.11.3.066.

[105] J. V. Stokman, *Generalized Onsager algebras*, Algebras Represent. Theory **23**, 1523 (2020), doi:10.1007/s10468-019-09903-6.

[106] Y. Miao, *Generalised Onsager algebra in quantum lattice models*, SciPost Phys. **13**, 070 (2022), doi:10.21468/SciPostPhys.13.3.070.

[107] P. Fendley, *Free fermions in disguise*, J. Phys. A: Math. Theor. **52**, 335002 (2019), doi:10.1088/1751-8121/ab305d.

[108] M. B. Hastings, *An area law for one-dimensional quantum systems*, J. Stat. Mech.: Theory Exp. P08024 (2007), doi:10.1088/1742-5468/2007/08/P08024.